NATIONAL ADVISORY COMMITTEE FOR AERONAUTICS

REPORT 942

INVESTIGATION IN THE LANGLEY 19-FOOT PRESSURE TUNNEL OF TWO WINGS OF NACA 65-210 AND 64-210 AIRFOIL SECTIONS WITH VARIOUS TYPE FLAPS

By JAMES C. SIVELLS and STANLEY H. SPOONER

1949

For sale by the Superintendent of Documents, U. S. Government Printing Office, Washington 25, D. C. Yearly subscription, $3; foreign, $4.50; single copy price varies according to size. - - - - - - - - - Price 25 cents

AERONAUTIC SYMBOLS

1. FUNDAMENTAL AND DERIVED UNITS

	Symbol	Metric		English	
		Unit	Abbreviation	Unit	Abbreviation
Length	l	meter	m	foot (or mile)	ft (or mi)
Time	t	second	s	second (or hour)	sec (or hr)
Force	F	weight of 1 kilogram	kg	weight of 1 pound	lb
Power	P	horsepower (metric)		horsepower	hp
Speed	V	kilometers per hour	kph	miles per hour	mph
		meters per second	mps	feet per second	fps

2. GENERAL SYMBOLS

W Weight$=mg$

g Standard acceleration of gravity$=9.80665$ m/s^2 or 32.1740 ft/sec^2

m Mass$=\frac{W}{g}$

I Moment of inertia$=mk^2$. (Indicate axis of radius of gyration k by proper subscript.)

μ Coefficient of viscosity

ν Kinematic viscosity

ρ Density (mass per unit volume)

Standard density of dry air, 0.12497 kg-m^{-4}-s^2 at 15° C and 760 mm; or 0.002378 lb-ft^{-4} sec^2

Specific weight of "standard" air, 1.2255 kg/m^3 or 0.07651 lb/cu ft

3. AERODYNAMIC SYMBOLS

S Area

S_w Area of wing

G Gap

b Span

c Chord

A Aspect ratio, $\frac{b^2}{S}$

V True air speed

q Dynamic pressure, $\frac{1}{2}\rho V^2$

L Lift, absolute coefficient $C_L=\frac{L}{qS}$

D Drag, absolute coefficient $C_D=\frac{D}{qS}$

D_0 Profile drag, absolute coefficient $C_{D_0}=\frac{D_0}{qS}$

D_i Induced drag, absolute coefficient $C_{D_i}=\frac{D_i}{qS}$

D_p Parasite drag, absolute coefficient $C_{D_p}=\frac{D_p}{qS}$

C Cross-wind force, absolute coefficient $C_c=\frac{C}{qS}$

i_w Angle of setting of wings (relative to thrust line)

i_t Angle of stabilizer setting (relative to thrust line)

Q Resultant moment

Ω Resultant angular velocity

R Reynolds number, $\rho\frac{Vl}{\mu}$ where l is a linear dimension (e.g., for an airfoil of 1.0 ft chord, 100 mph, standard pressure at 15° C, the corresponding Reynolds number is 935,400; or for an airfoil of 1.0 m chord, 100 mps, the corresponding Reynolds number is 6,865,000)

α Angle of attack

ϵ Angle of downwash

α_0 Angle of attack, infinite aspect ratio

α_i Angle of attack, induced

α_a Angle of attack, absolute (measured from zero-lift position)

γ Flight-path angle

REPORT 942

INVESTIGATION IN THE LANGLEY 19-FOOT PRESSURE TUNNEL OF TWO WINGS OF NACA 65-210 AND 64-210 AIRFOIL SECTIONS WITH VARIOUS TYPE FLAPS

By JAMES C. SIVELLS and STANLEY H. SPOONER

Langley Aeronautical Laboratory
Langley Air Force Base, Va.

National Advisory Committee for Aeronautics

Headquarters, 1724 F Street NW., Washington 25, D. C.

Created by act of Congress approved March 3, 1915, for the supervision and direction of the scientific study of the problems of flight (U. S. Code, title 50, sec. 151). Its membership was increased from 12 to 15 by act approved March 2, 1929, and to 17 by act approved May 25, 1948. The members are appointed by the President, and serve as such without compensation.

TECHNICAL COMMITTEES

AERODYNAMICS
POWER PLANTS FOR AIRCRAFT
AIRCRAFT CONSTRUCTION
OPERATING PROBLEMS
INDUSTRY CONSULTING

Coordination of Research Needs of Military and Civil Aviation
Preparation of Research Programs
Allocation of Problems
Prevention of Duplication
Consideration of Inventions

LANGLEY AERONAUTICAL LABORATORY
Langley Field, Va.

LEWIS FLIGHT PROPULSION LABORATORY
Cleveland Airport, Cleveland, Ohio

AMES AERONAUTICAL LABORATORY
Moffett Field, Calif.

Conduct, under unified control, for all agencies of scientific research on the fundamental problems of flight

---

OFFICE OF AERONAUTICAL INTELLIGENCE
Washington, D. C.

Collection, classification, compilation, and dissemination of scientific and technical information on aeronautics

REPORT 942

INVESTIGATION IN THE LANGLEY 19-FOOT PRESSURE TUNNEL OF TWO WINGS OF NACA 65-210 AND 64-210 AIRFOIL SECTIONS WITH VARIOUS TYPE FLAPS

By James C. Sivells and Stanley H. Spooner

SUMMARY

An investigation has been conducted in the Langley 19-foot pressure tunnel to determine the maximum lift and stalling characteristics of two thin wings equipped with several types of flaps. Split, single slotted, and double slotted flaps were tested on one wing which had NACA 65–210 airfoil sections and split and double slotted flaps were tested on the other, which had NACA 64–210 airfoil sections. Both wings had zero sweep, an aspect ratio of 9, and a taper ratio of 0.4.

At a Reynolds number of 4,400,000 each type of flap increased the maximum lift coefficients of the two wings by increments which were approximately proportional to the flap neutral values of 1.21 and 1.35 for the NACA 65–210 wing and the NACA 64–210 wing, respectively. The values of maximum lift coefficient for the wings with full-span double slotted flaps were 2.48 and 2.76, which values represent increments of 105 percent of the flap neutral values. The addition of a representative fuselage or leading-edge roughness was more detrimental to the NACA 64–210 wing, but its values of maximum lift coefficient were still consistently higher than those of the NACA 65–210 wing. The values of maximum lift coefficient increased with increasing Reynolds numbers up to a value of 4,400,000. Above this value, the test Mach number was high enough so that the effects of compressibility appeared to cause the values of maximum lift coefficient to increase less rapidly or to decrease with increasing Reynolds numbers.

The stall of the NACA 64–210 wing was somewhat more abrupt but slightly farther inboard than that of the NACA 65–210 wing. The pattern of the stall was approximately the same for all flap configurations with or without leading-edge roughness. The main effect of roughness was to make the stall progression more gradual. The fuselage, however, caused the stall to begin inboard near the wing-fuselage junction.

INTRODUCTION

The wing sections of an airplane capable of flying at high subsonic speeds must be relatively thin in order to delay the onset of the effects of compressibility. These thin sections, however, cannot normally develop as high values of maximum lift coefficient as thicker sections used on slower airplanes. More powerful high lift flaps must therefore be used on high-speed airplanes to obtain landing characteristics approaching those of lower-speed, but otherwise comparable, airplanes. In order to develop high lift flaps suitable for thin airfoils, an investigation was conducted in the Langley two-dimensional low-turbulence tunnels. (See references 1 and 2.) The most promising results of this investigation were incorporated in the design of two thin wings, the three-dimensional characteristics of which were investigated in the Langley 19-foot pressure tunnel.

One of these wings had NACA 65–210 airfoil sections and was equipped with split, single slotted, and double slotted flaps. The other wing had NACA 64–210 airfoil sections and was equipped with split and double slotted flaps. The plan form of both wings was typical of a long-range airplane in that the aspect ratio was 9 and the taper ratio was 0.4. Presented herein are the results of tests made at relatively high Reynolds numbers to determine the maximum lift and stalling characteristics of these two wings with partial-span and full-span flaps both with and without a representative fuselage and leading-edge roughness.

COEFFICIENTS AND SYMBOLS

The coefficients and symbols used herein are defined as follows:

C_L	lift coefficient (L/qS)
C_D	drag coefficient (D/qS)
C_m	pitching-moment coefficient ($M/qS\bar{c}$)
$C_{L_{trim}}=C_L+\frac{C_m}{3}$	(Tail length$=3\bar{c}$)
$C_{L_{max}}$	maximum lift coefficient
$\Delta C_{L_{max}}$	increment in $C_{L_{max}}$ due to flaps

where

L	lift
D	drag
M	pitching moment about $0.25\bar{c}$
q	dynamic pressure of free stream $\left(\frac{1}{2}\rho V^2\right)$
S	wing area (24.94 ft^2)
$\bar{c}$	mean aerodynamic chord (1.769 ft) $\left(\frac{2}{S}\int_0^{b/2} c^2\,dy\right)$
ρ	mass density of air
V	airspeed
V_v	vertical velocity in glide
c	local wing chord
b	wing span (15 ft)
y	spanwise coordinate

and

α	corrected angle of attack of root chord
R	Reynolds number ($\rho V\bar{c}/\mu$)
M	Mach number (V/a)
μ	coefficient of viscosity
a	sonic velocity

MODELS AND TESTS

The two wings were constructed of solid steel and were geometrically similar except that one was contoured to NACA 65–210 airfoil sections and the other to NACA 64–210 airfoil sections. The taper ratio was 0.4 and the aspect ratio was 9. The sweep and dihedral at the 0.25-chord line were 0° and 3°, respectively. Both wings were uniformly twisted about the 0.25-chord line to produce 2° washout. A mahogany fuselage was attached to the wings for some of the tests. The wing and fuselage mounted in the Langley 19-foot pressure tunnel are shown in figure 1, and the general dimensions of the models are given in figure 2.

The wing with NACA 65–210 airfoil sections was tested with partial-span and full-span split, single slotted, and double slotted flaps. The wing with NACA 64–210 airfoil sections was tested with partial-span and full-span split and double slotted flaps. The split and single slotted flaps were, respectively, 20 and 25 percent of the local wing chord. The double slotted flap was comprised of a 7.5-percent-chord vane and a 25-percent-chord main flap. For the NACA 65–210 wing, the single slotted flap was used as the main flap of the double slotted flap. The same vane ordinates were used for both wings. The ordinates for the airfoil sections and flaps are given in tables I to V. A finite trailing-edge thickness of 1 percent of the maximum thickness was arbitrarily set for these wings. It was not possible in the construction of the wings to make the flap wells deep enough to allow the double slotted flaps to be retracted. Unpublished two-dimensional data indicated that the difference in depth and shape of the double-slotted-flap well and that of the single-slotted-flap well would not affect the test results inasmuch as the flap-well ordinates in the vicinity of the deflected vane were approximately the same. For these wings, therefore, the flap wells for single slotted flaps were constructed according to the ordinates of table VI and were not changed for the double-slotted-flap tests.

The split, single slotted, and double slotted flaps were deflected 60°, 45°, and 50°, respectively, for these tests. The flap positions used are shown in figure 3 and were determined to be optimum from preliminary two-dimensional tests. These positions do not completely conform with the final optimum values given in references 1 and 2. The partial-span flaps extended to 60 percent of the semispan and the full-span flaps, to 97.5 percent. For most of the tests of the wings without the fuselage, the flaps extended inboard to the plane of symmetry. A few tests of the NACA 65–210 wing with the fuselage off were made in which the flaps extended inboard only as far as they did when the fuselage was attached.

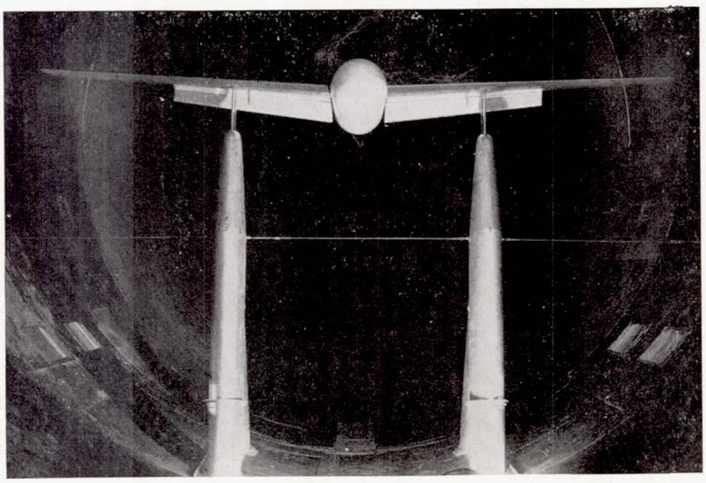

(a) Front view.

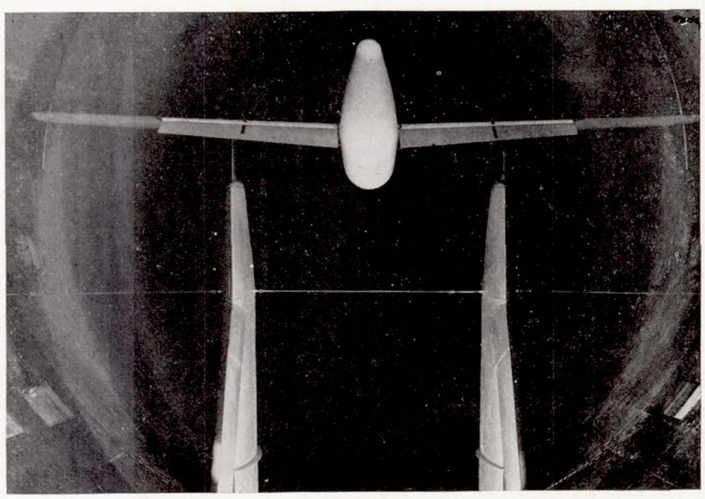

(b) Rear view.

FIGURE 1.—Wing with fuselage mounted in Langley 19-foot pressure tunnel. Partial-span double-slotted-flap configuration.

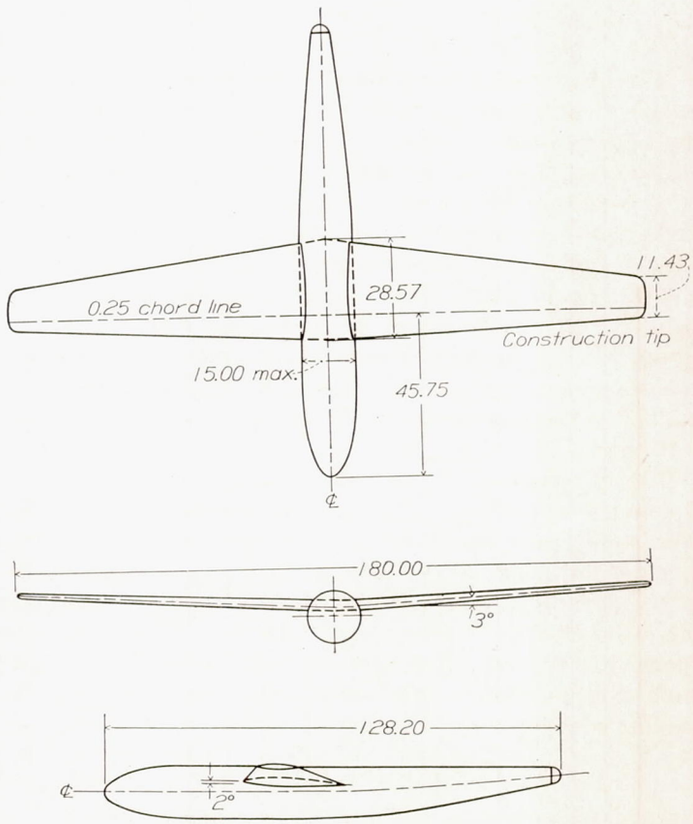

FIGURE 2.—Wing and fuselage for tests in Langley 19-foot pressure tunnel. Root chord line at 0.25c is 2.625 inches above fuselage center line; wing area, 24.94 sq. ft.; aspect ratio, 9.02; washout, 2°; taper ratio, 0.4. (All dimensions are in inches.)

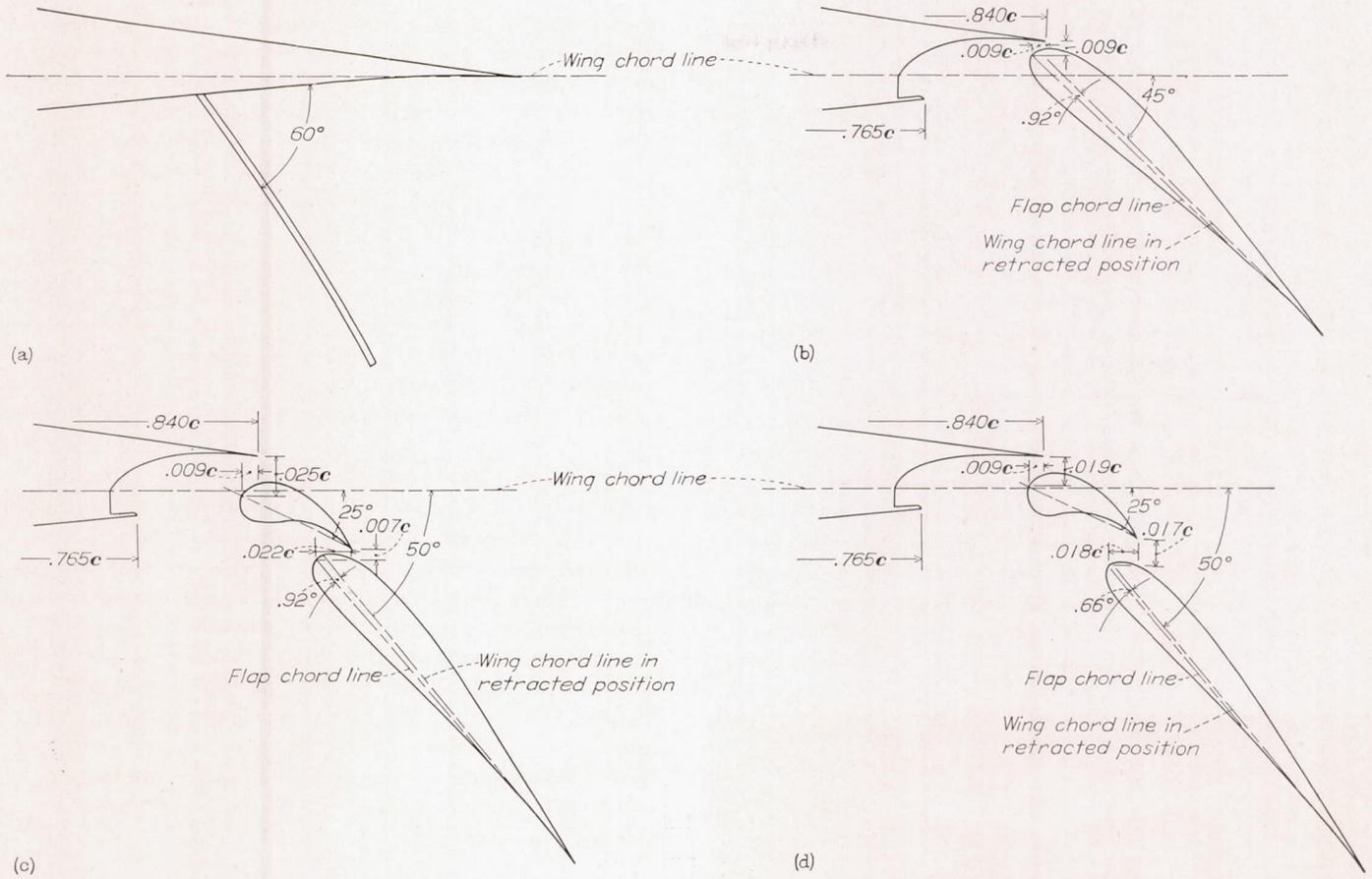

(a) Split flap; NACA 65–210 and 64–210 wings.
(b) Single slotted flap; NACA 65–210 wing.
(c) Double slotted flap; NACA 65–210 wing.
(d) Double slotted flap; NACA 64–210 wing.

FIGURE 3.—Details of flaps.

The models used for the tests reported herein were found to be smooth and fair and conformed with the true airfoil contours to within 0.003 inch over the forward 30 percent of the wing and within 0.008 inch over the rearward areas.

The tests were conducted with the air in the tunnel compressed to approximately 34 pounds per square inch absolute pressure. The majority of the tests were made at a dynamic pressure of 85 pounds per square foot, corresponding to a Reynolds number of approximately 4,400,000 and a Mach number of about 0.17. Scale-effect tests were made over a range of Reynolds number from 3,200,000 to 6,400,000 corresponding to a range of Mach number from 0.12 to 0.24.

The aerodynamic forces and moments were measured by a simultaneously recording, six-component balance system. The stalling characteristics were determined from observations of the behavior of tufts attached to the upper surface of the model behind the 0.30-chord line. In order to determine the effect of leading-edge roughness, tests were made with No. 60 carborundum grains applied to the nose of each wing over a surface length of 0.08 chord measured from the leading edge on both surfaces.

RESULTS AND DISCUSSION

All data have been reduced to standard nondimensional coefficients. Corrections have been applied to the force and moment data to account for the tare and interference effects of the model support system. Stream-angle and jet-boundary corrections have been applied to the angle of attack and to the drag coefficients.

The lift, drag, and pitching-moment coefficients of the two wings are shown in figures 4 to 13 for a Reynolds number of 4,400,000. A comparison of the various flap configurations is made in figure 14 for the wing-fuselage combination. The effects of Reynolds number on maximum lift coefficient are given in figures 15, 16, and 17. The stalling characteristics are given in figures 18 to 29. The values of the trimmed and untrimmed maximum lift coefficients of the various flap configurations are summarized in table VII.

Some inconsistency can be noted in the values of maximum lift coefficient for the various configurations. This inconsistency appears to be a characteristic of these thin wings. Preliminary tests of these wings showed that very small errors in airfoil contour, particularly around the leading edge, could cause large changes in the stalling angle of attack and the resulting value of maximum lift coefficient. For the tests described herein, the airfoil contours were held to very close tolerances and extreme care was taken during the course of the smooth-wing tests to keep the wings in as nearly perfect condition as possible. In spite of all precautions taken, some inconsistency still appears in the results and, therefore, some of the effects of model configuration and Reynolds number may be somewhat obscured.

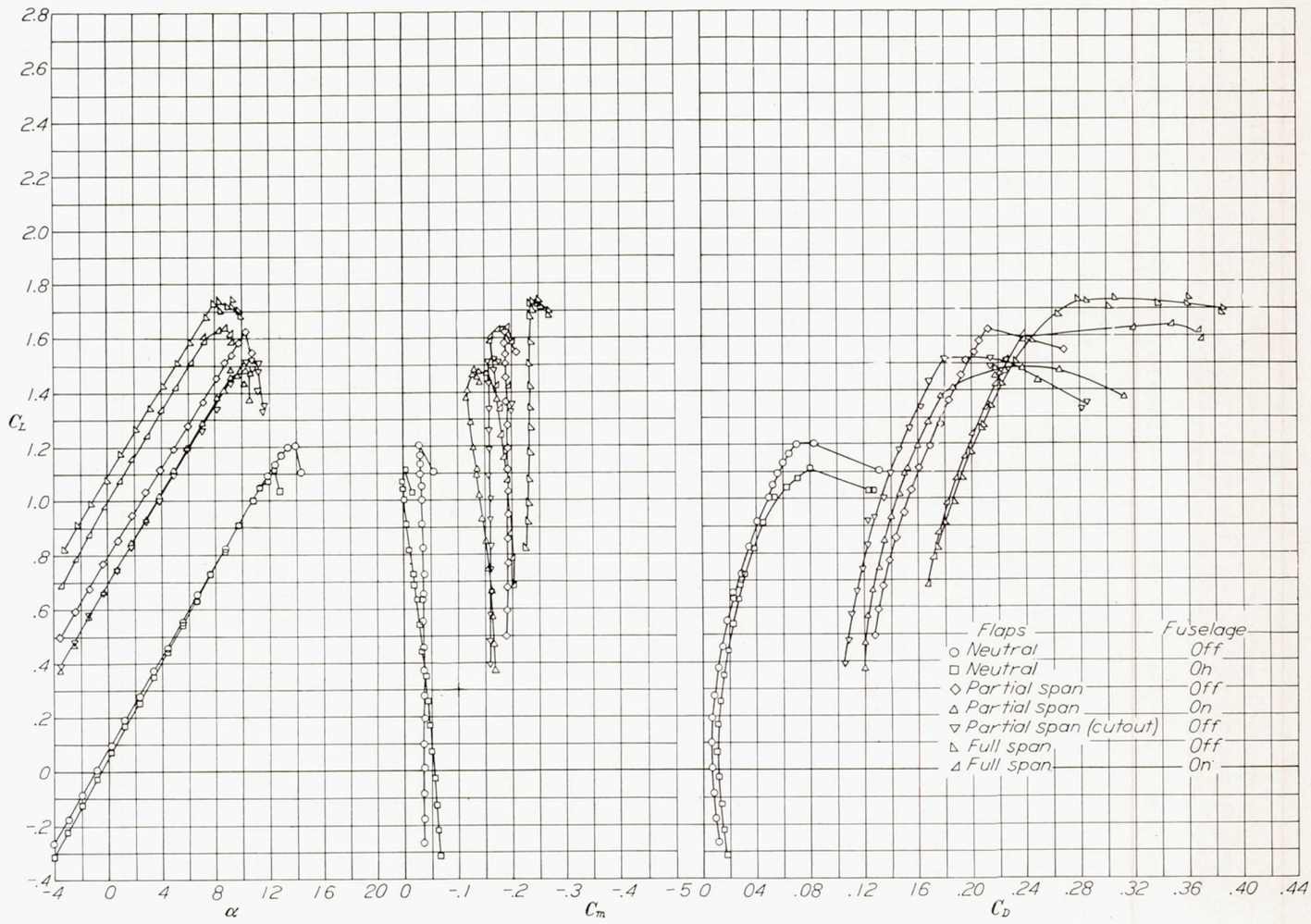

FIGURE 4.—Aerodynamic characteristics of NACA 65–210 wing with and without split flaps and fuselage. $R \approx$ 4,400,000; $M \approx 0.17$.

FLAP EFFECTIVENESS

If the values of maximum lift coefficient of the wings with flaps are expressed in percent of the flap neutral values, the flap effectiveness for both wings was practically the same at a Reynolds number of 4,400,000. Inasmuch as the flap neutral value for the NACA 64–210 wing was 1.35 as compared with 1.21 for the NACA 65–210 wing, the flap extended values for the NACA 64–210 wing were consistently higher. The increments in maximum lift coefficient due to flaps for the smooth-wing condition and for a Reynolds number of 4,400,000 are as follows:

Flap type	Flap span	$\Delta C_{L_{max}}$		$\Delta C_{L_{max}}$ in percent of flap neutral value
		NACA 65–210 wing	NACA 64–210 wing	
Split	Partial	0.42	0.52	35 to 38
	Full	.53	.59	44
Slotted	Partial	.66		55
	Full	.94		78
Double slotted	Partial	.89	1.07	74 to 79
	Full	1.27	1.41	105

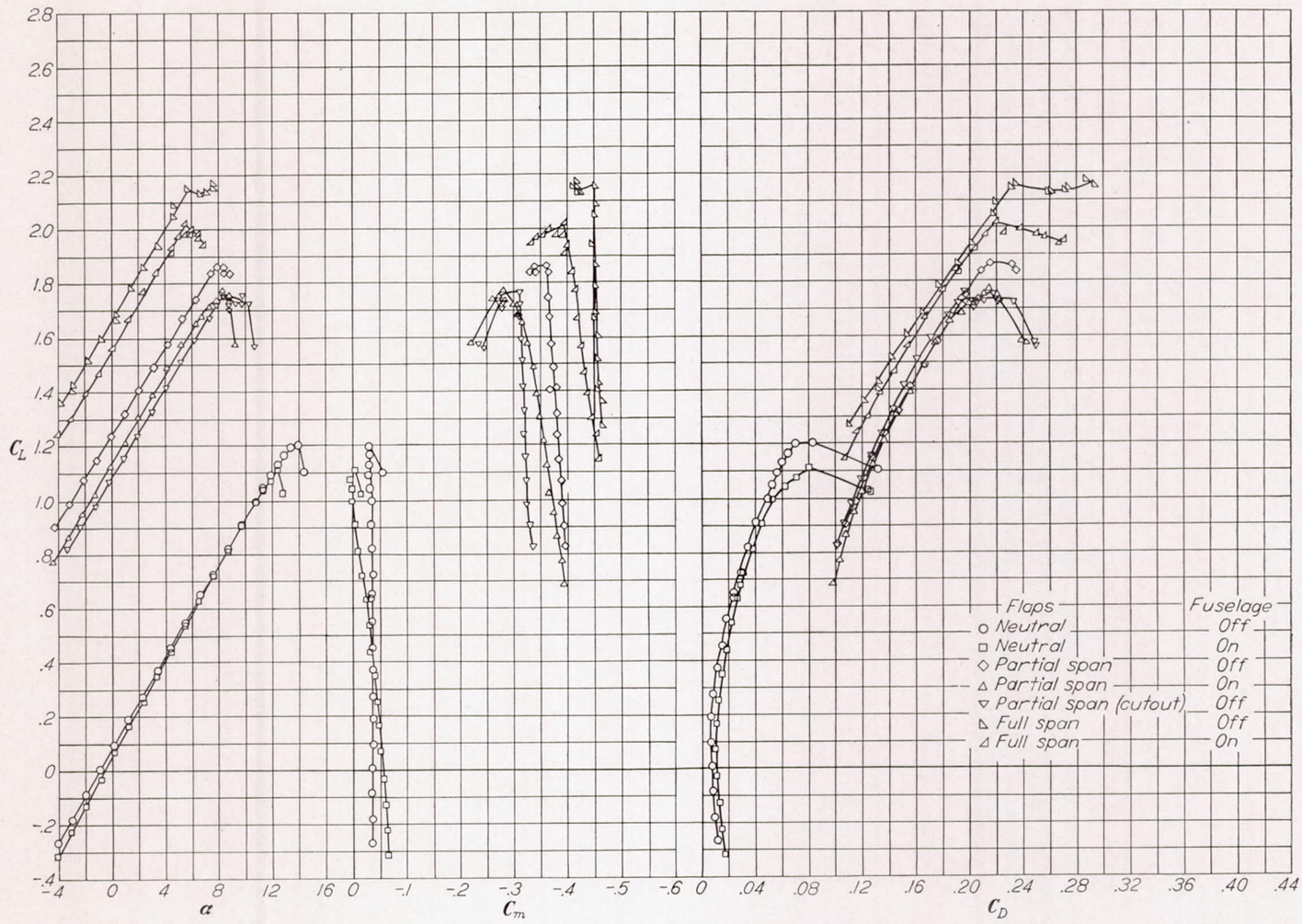

FIGURE 5.—Aerodynamic characteristics of NACA 65-210 wing with and without single slotted flaps and fuselage. $R \approx 4{,}400{,}000$; $M \approx 0.17$.

These increments are of the order of magnitude that would be expected from the two-dimensional data of references 1 and 2 although the flap positions were not quite the same.

The single slotted and double slotted flaps had the effect of producing an unstable break in the pitching-moment curves at $C_{L_{max}}$. This effect is a section characteristic since it was also noted in reference 2. Inasmuch as the stall of these wings tends to begin inboard with the fuselage in place, as is shown subsequently, the decrease in downwash accompanying the stall produces a positive increment of lift on the tail of a complete airplane and thereby tends to compensate for the unstable break.

In order to compare the effects of the various types of flaps on the landing characteristics of a typical airplane, contours of constant gliding speed and constant vertical (sinking) speed are superimposed on the fuselage-on drag polars in figure 14. In this figure the lift of the tail necessary to trim the airplane is taken into account in the lift coefficient presented $(C_{L_{trim}})$. For this purpose a tail length of three times the mean aerodynamic chord was assumed and the center of gravity of the airplane was assumed to be located at the quarter-chord point of the mean aerodynamic chord. For the constant-speed contours a wing loading of 60 pounds per square foot was assumed and standard sea-level conditions were used. Obviously, the drag of nacelles, landing gear, tail, and protuberances are not shown on this figure nor are

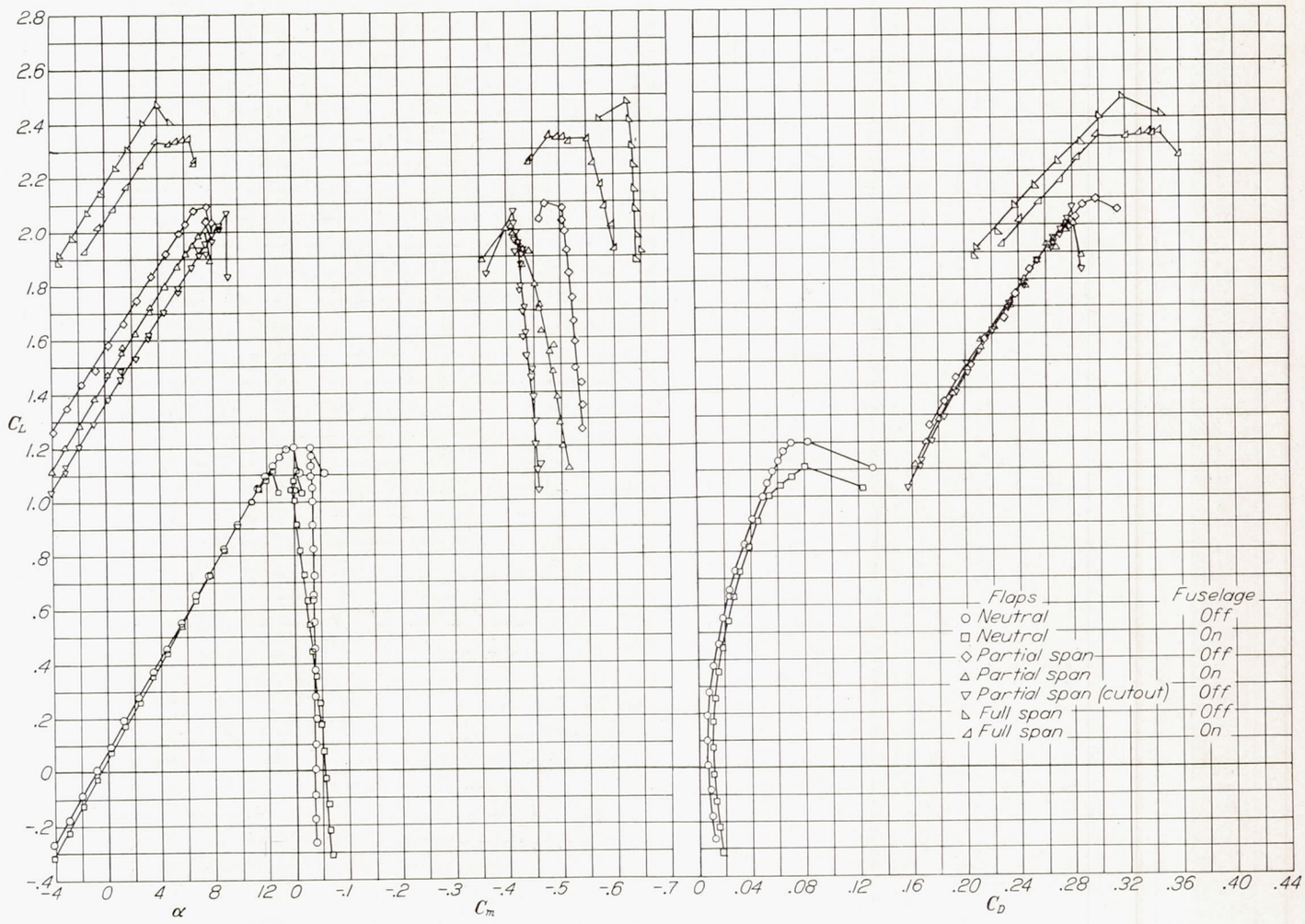

FIGURE 6.—Aerodynamic characteristics of NACA 65–210 wing with and without double slotted flaps and fuselage. $R \approx 4{,}400{,}000$; $M \approx 0.17$.

the effects of power. The relative effects of the types of flaps and the flap span, however, are readily shown. The single-slotted-flap configuration has the lowest sinking speed of any of the flapped configurations but a higher gliding speed than the double-slotted-flap configuration. Increasing the flap span from partial to full span decreases the sinking speed for the single-slotted-flap and double-slotted-flap configurations because of the lower induced drag but increases the sinking speed for the split-flap configuration because of the high profile drag of split flaps.

EFFECT OF FUSELAGE

The reduction in maximum lift coefficient caused by the fuselage was approximately 0.1 for the NACA 65–210 wing and varied from 0.1 to 0.3 for the NACA 64–210 wing. The values of maximum lift coefficient, however, were still higher for the NACA 64–210 wing than for the NACA 65–210 wing. Since the tests were conducted with no fillets at the wing-fuselage junction, properly designed fillets might have minimized the loss in maximum lift.

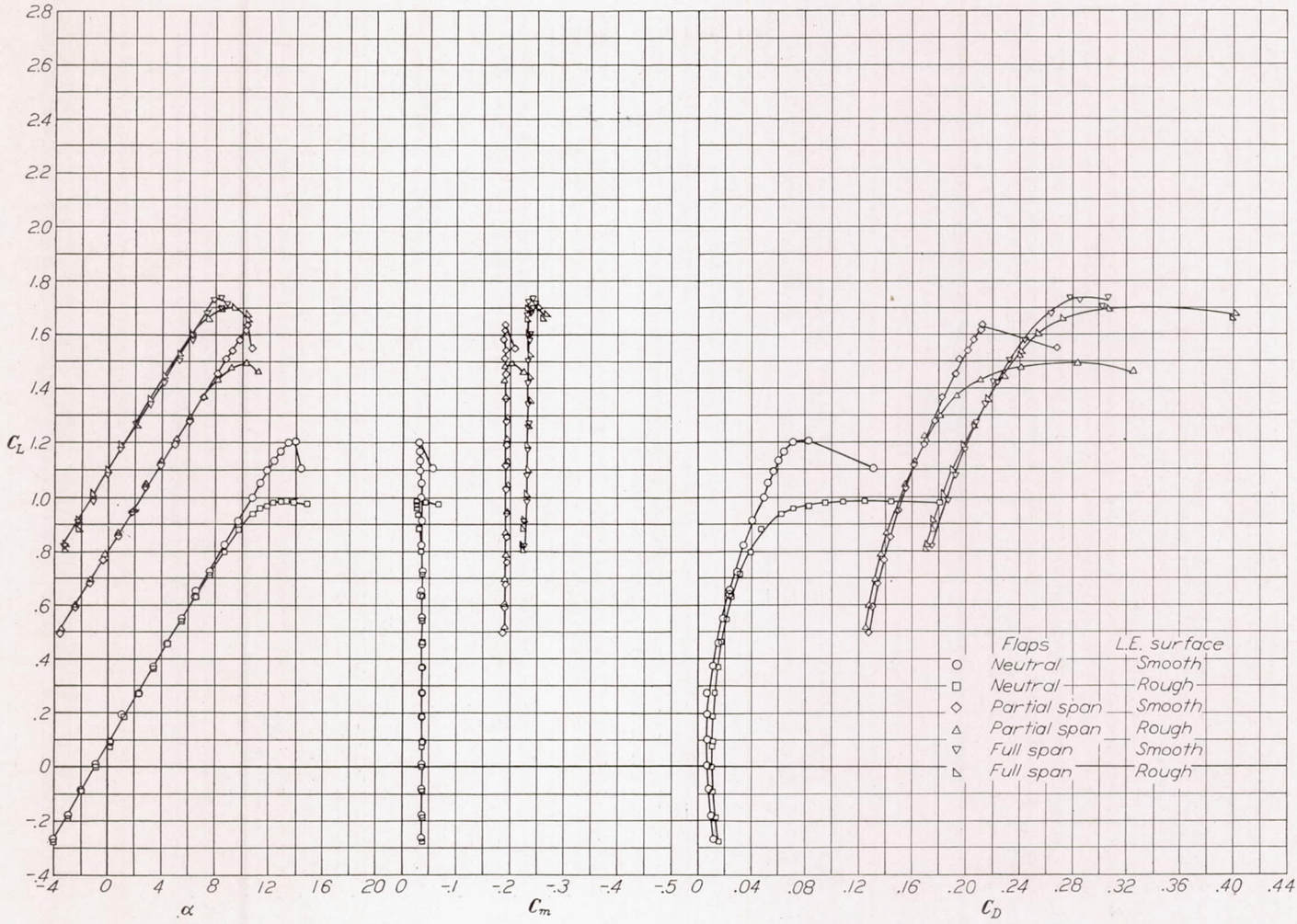

FIGURE 7.—Aerodynamic characteristics of NACA 65–210 wing with and without split flaps and leading-edge roughness. $R \approx 4{,}400{,}000$; $M \approx 0.17$.

The results of the tests of the NACA 65–210 wing with the flaps removed from that part of the wing normally occupied by the fuselage are shown in figures 4 to 6. The data in the linear lift-curve range indicate that some of the lift due to the single slotted and double slotted flaps was carried across the fuselage, whereas practically none of the lift due to the split flaps was carried across.

For all configurations the fuselage caused a destabilizing effect on the pitching moment equal to a forward shift of the aerodynamic center of about 5 percent of the mean aerodynamic chord.

EFFECT OF LEADING-EDGE ROUGHNESS

Leading-edge roughness caused a rounding of the lift-curve peaks and a reduction in the maximum lift coefficients of both wings with and without flaps. The reduction usually amounted to about 0.2 for the NACA 65–210 wing and about 0.3 for the NACA 64–210 wing. As was true for the fuselage configuration, the maximum lift coefficients of the NACA 64–210 wing were higher than those of the NACA 65–210 wing even though the effect of roughness on the NACA 64–210 wing was greater.

865770—50——2

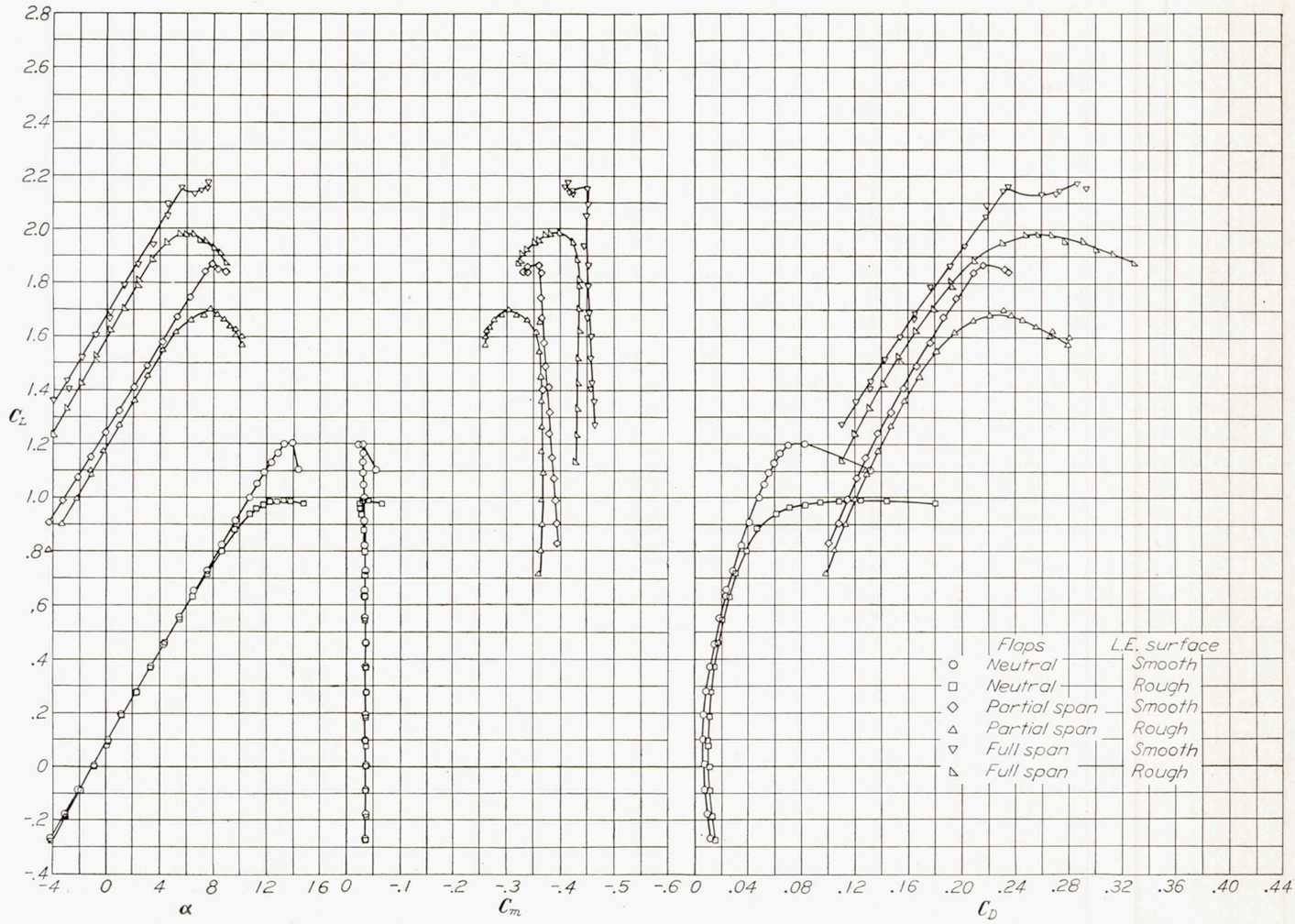

FIGURE 8.—Aerodynamic characteristics of NACA 65–210 wing with and without single slotted flaps and leading-edge roughness. $R \approx 4{,}000{,}000$; $M \approx 0.17$.

At low angles of attack, the addition of leading-edge roughness usually decreased the lift coefficient slightly. For the NACA 64–210 wing with double slotted flaps (fig. 13), the lift coefficient was increased by roughness and the pitching-moment coefficient was increased negatively. An inspection of the stalling characteristics (fig. 29) indicates that this effect may be due in part to the fact that the flap was unstalled for this condition but had some small stalled areas when the wing was smooth. Another contributing factor to this effect may have been that the support tare and interference corrections for the smooth wing were used to correct both smooth-wing and rough-wing data.

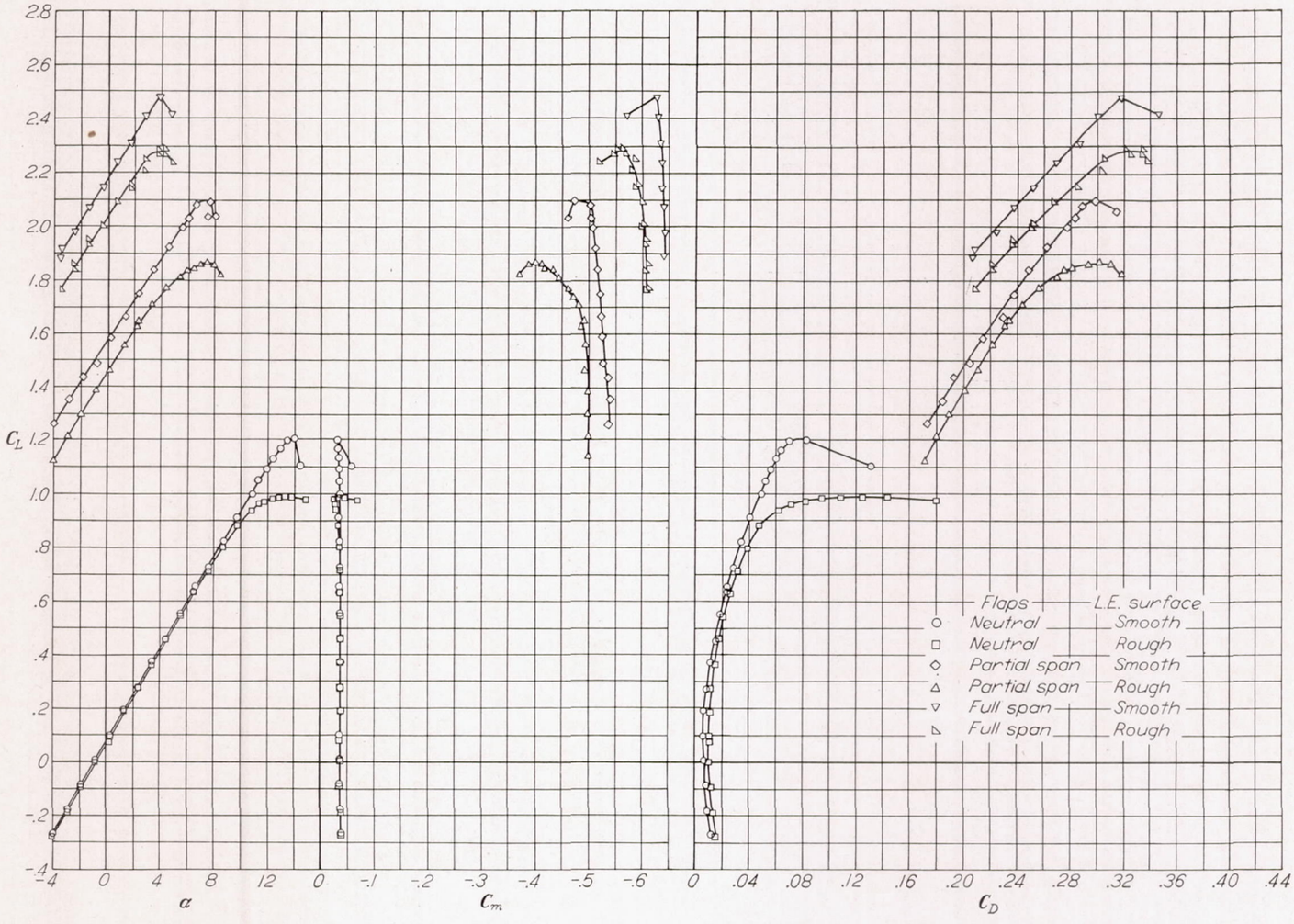

FIGURE 9.—Aerodynamic characteristics of NACA 65-210 wing with and without double slotted flaps and leading-edge roughness. $R \approx 4{,}400{,}000$; $M \approx 0.17$.

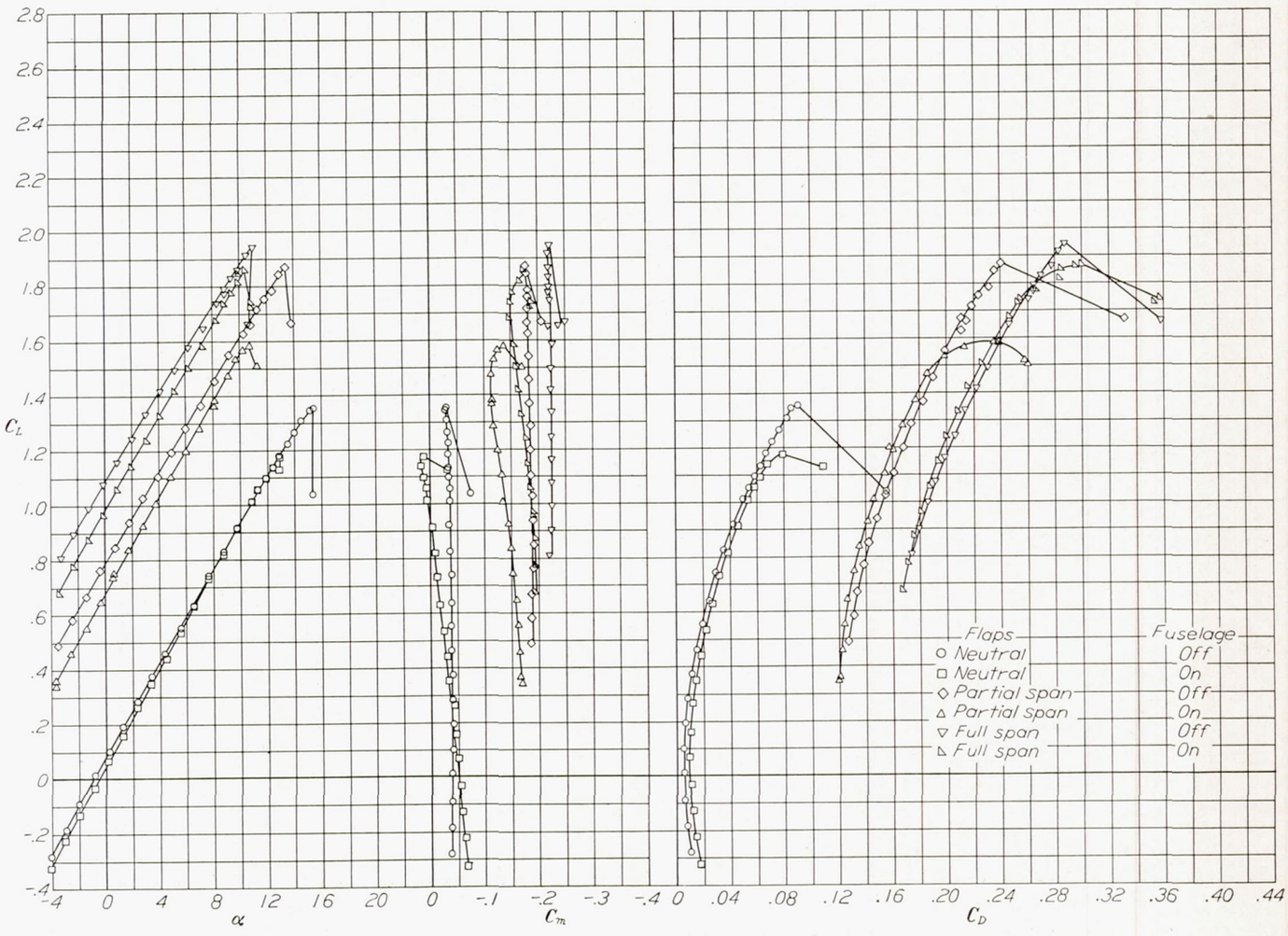

FIGURE 10.—Aerodynamic characteristics of NACA 64–210 wing with and without split flaps and fuselage. $R \approx$ 4,400,000; $M \approx$ 0.17.

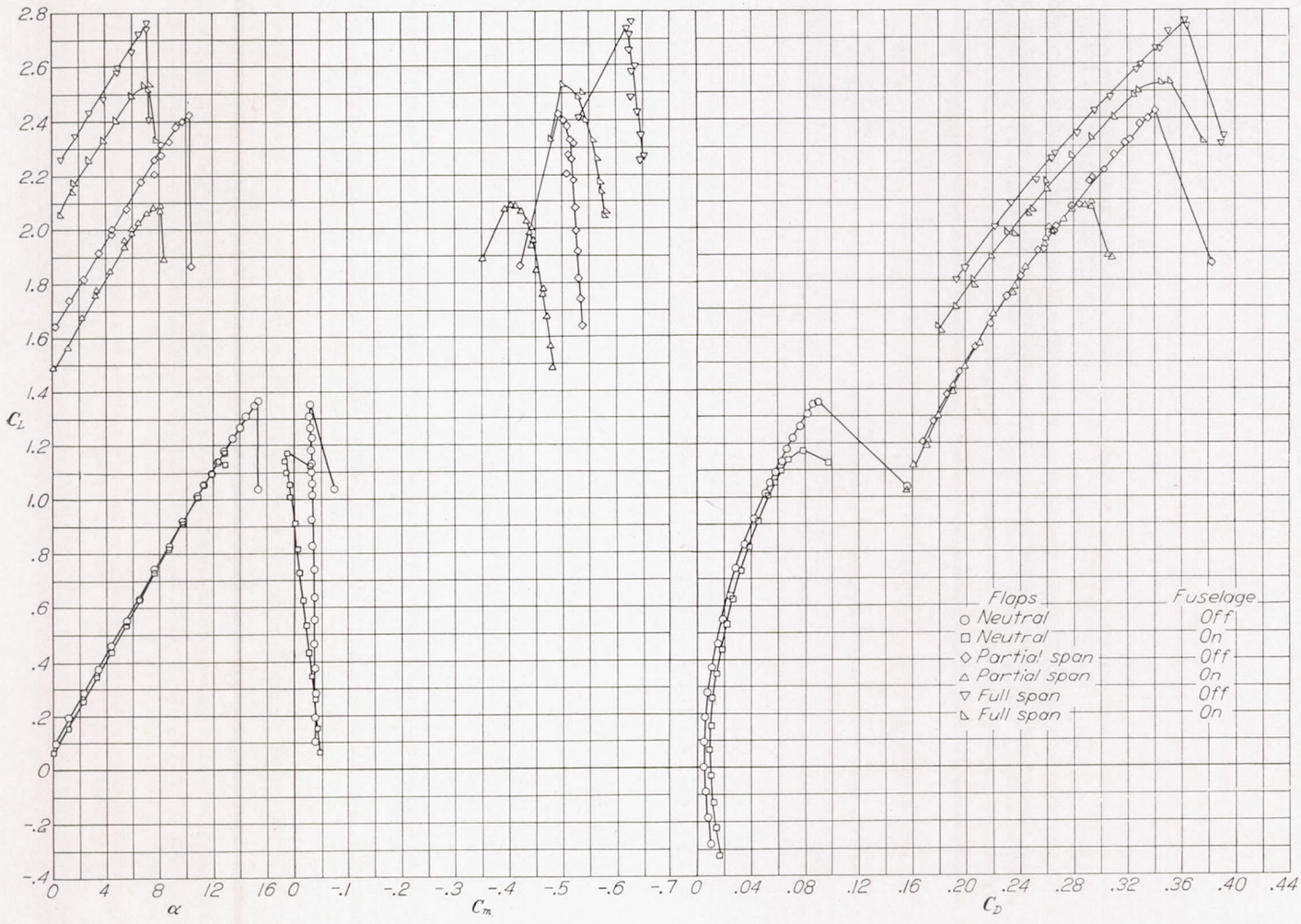

FIGURE 11.—Aerodynamic characteristics of NACA 64–210 wing with and without double slotted flaps and fuselage. $R \approx$ 4,400,000; $M \approx$ 0.17.

866770—50——3

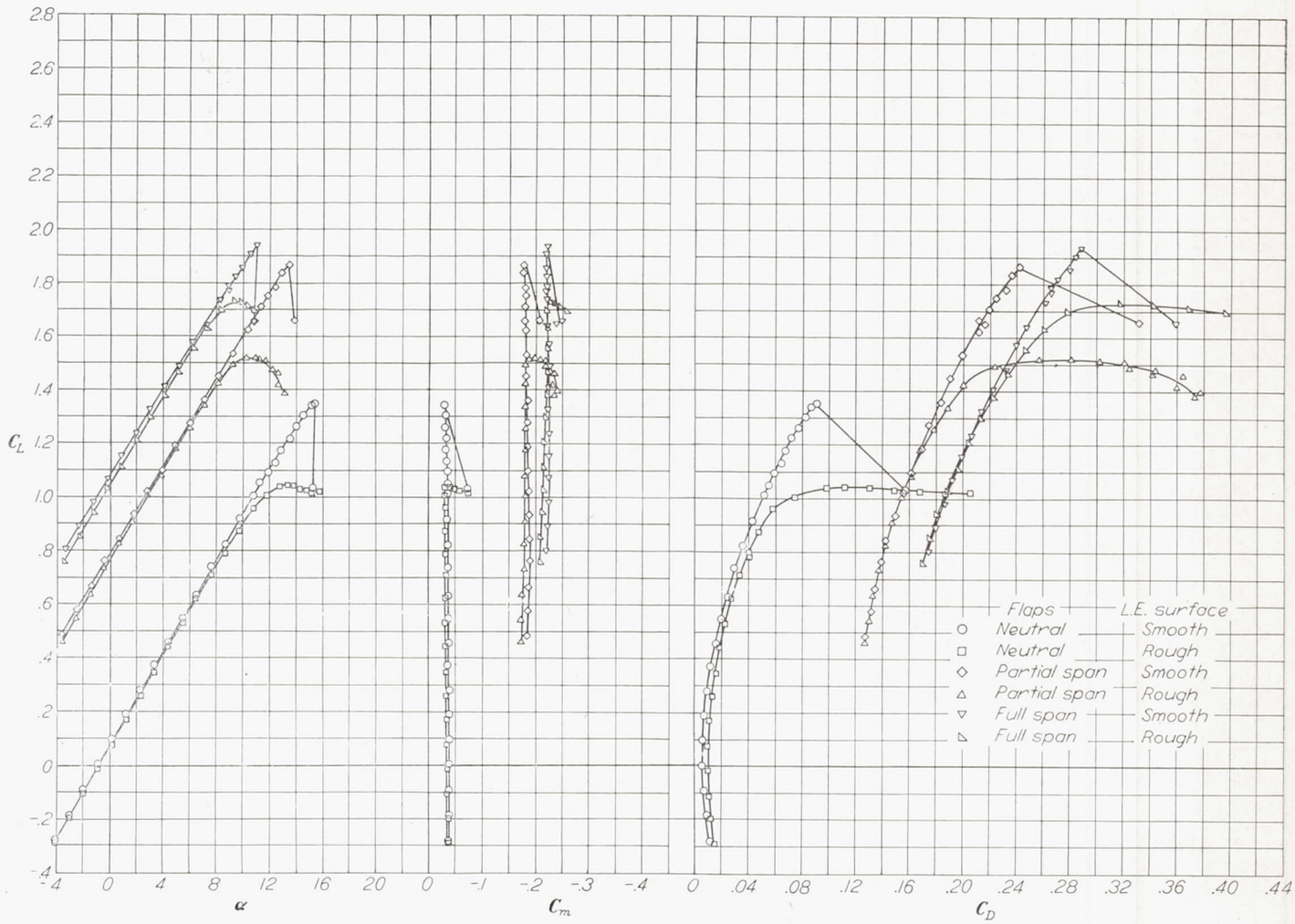

FIGURE 12.—Aerodynamic characteristics of NACA 64–210 wing with and without split flaps and leading-edge roughness. $R \approx 4{,}400{,}400$; $M \approx 0.17$.

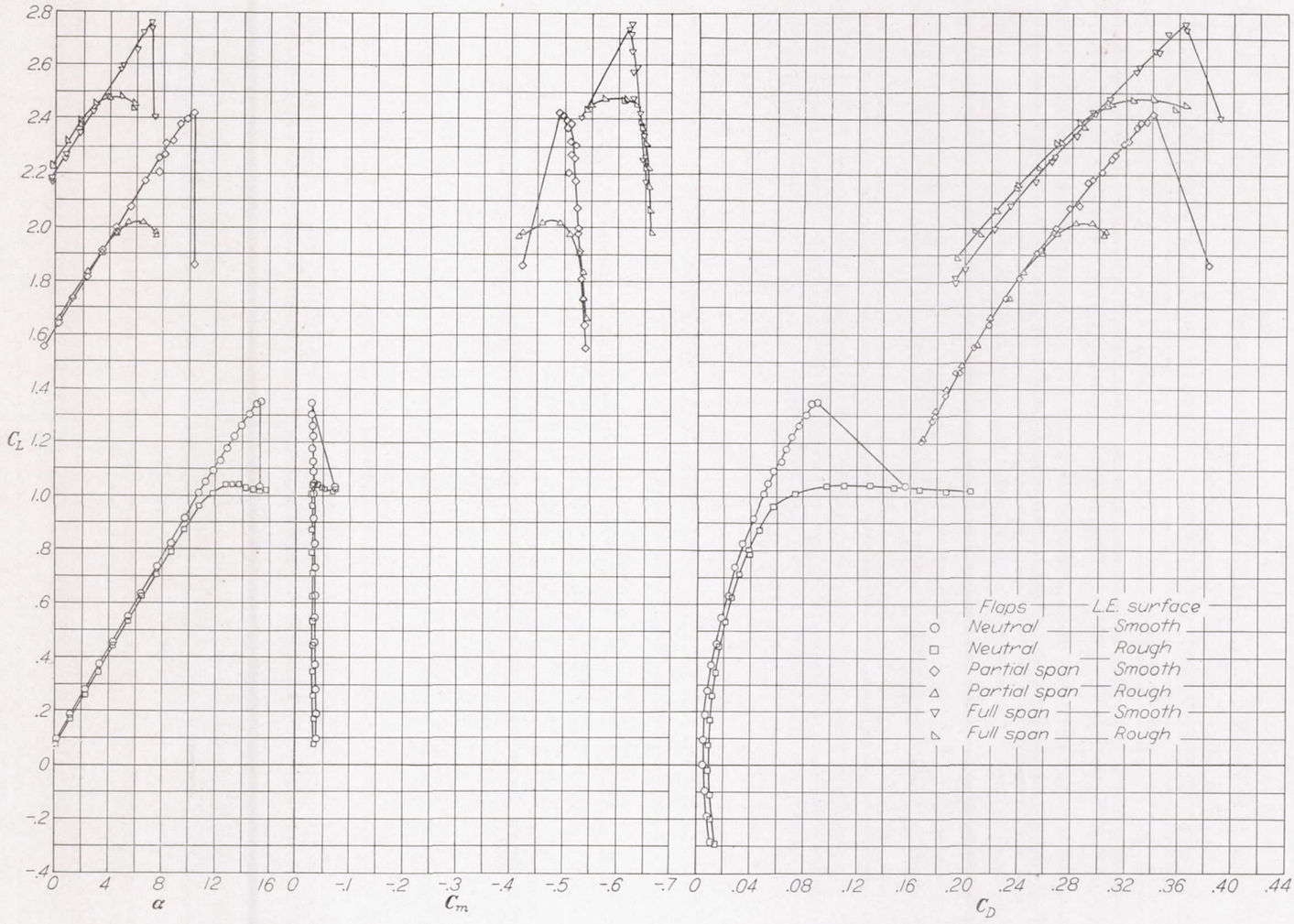

FIGURE 13.—Aerodynamic characteristics of NACA 64–210 wing with and without double slotted flaps and leading-edge roughness. $R \approx 4{,}400{,}000$; $M \approx 0.17$.

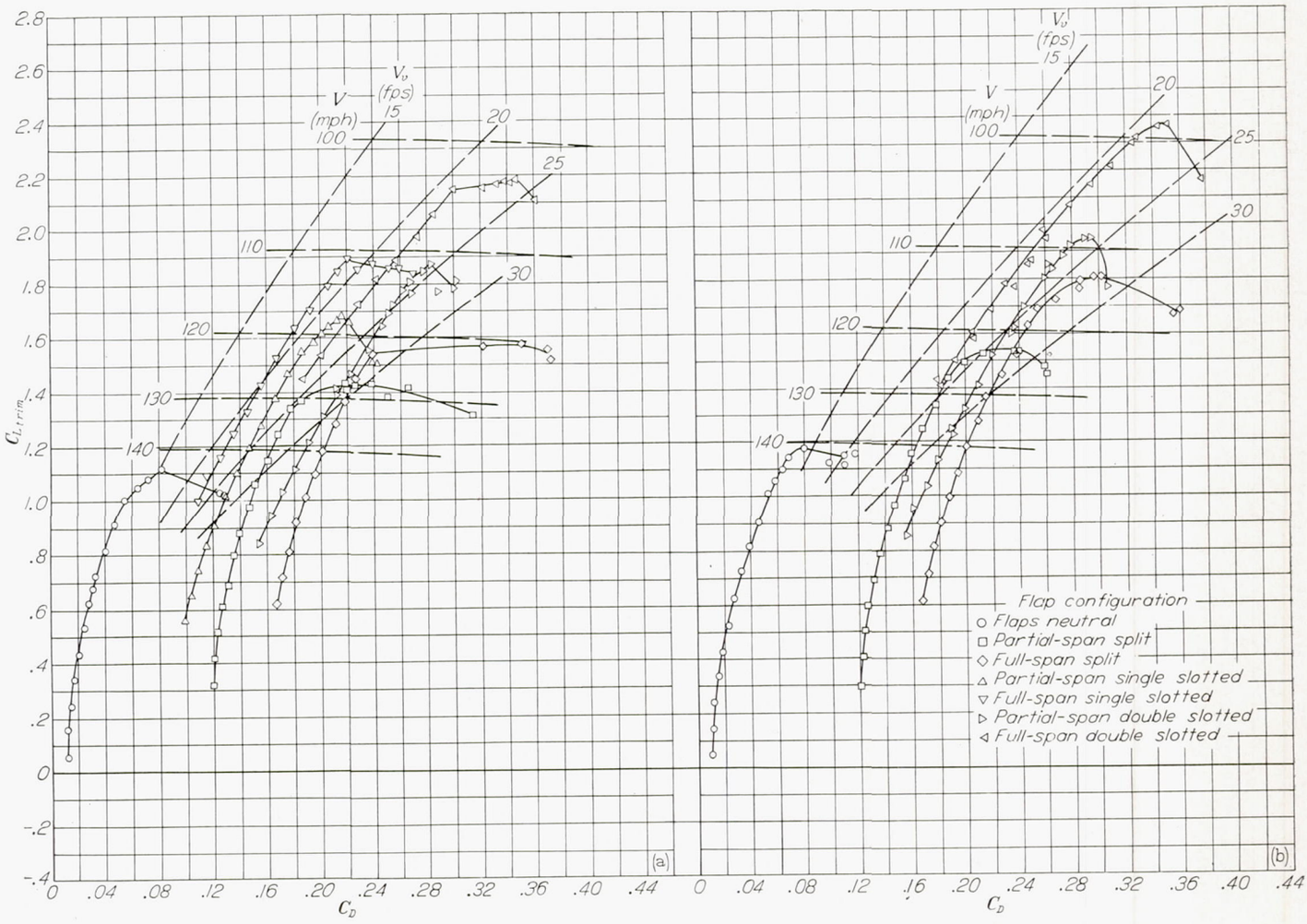

(a) NACA 65–210 wing with fuselage.

(b) NACA 64–210 wing with fuselage.

FIGURE 14.—Comparison of the effects of various flap configurations on the gliding characteristics of an airplane with a wing loading of 60 pounds per square foot; standard sea-level conditions.

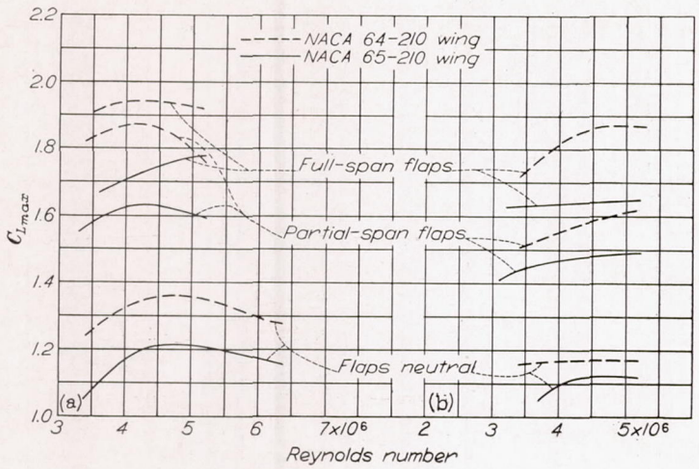

(a) Wing. (b) Wing with fuselage.

FIGURE 15.—Scale effect on NACA 65-210 and 64-210 wings with and without split flaps and fuselage.

SCALE EFFECT

The variation of maximum lift coefficient with Reynolds number is shown in figures 15, 16, and 17 for the various flap configurations. Although the data are not completely consistent, they show the same general trends which were indicated by the two-dimensional tests (references 1 and 2) if some allowance is made at the highest Reynolds numbers (Mach numbers about 0.2) for the effects of compressibility which are probably similar to those described in reference 3. In general, the maximum lift coefficients of both the NACA 65–210 and NACA 64–210 wings increased with increasing Reynolds number for Reynolds numbers below 4,400,000. Above this Reynolds number, the maximum lift coefficients increased less rapidly or decreased because of the effects of compressibility present for the three-dimensional tests.

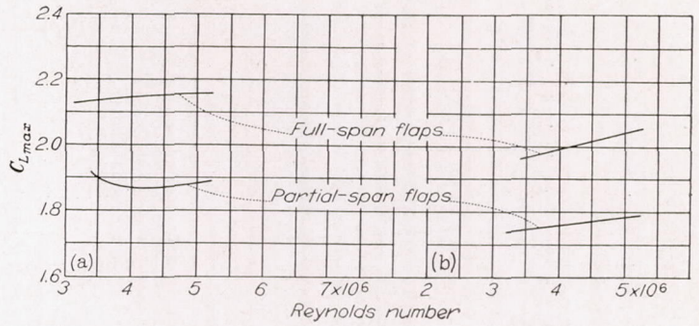

(a) Wing. (b) Wing with fuselage.

FIGURE 16.—Scale effect on NACA 65-210 wing with single slotted flaps with and without fuselage.

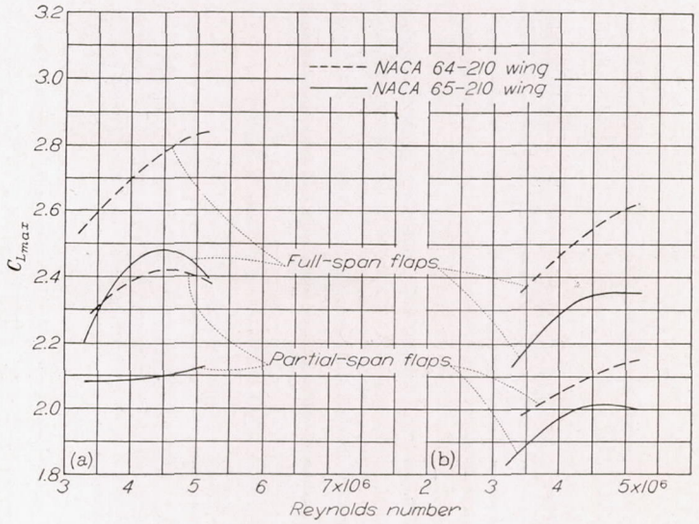

(a) Wing. (b) Wing with fuselage.

FIGURE 17.—Scale effect on NACA 65-210 and 64-210 wings with double slotted flaps with and without fuselage.

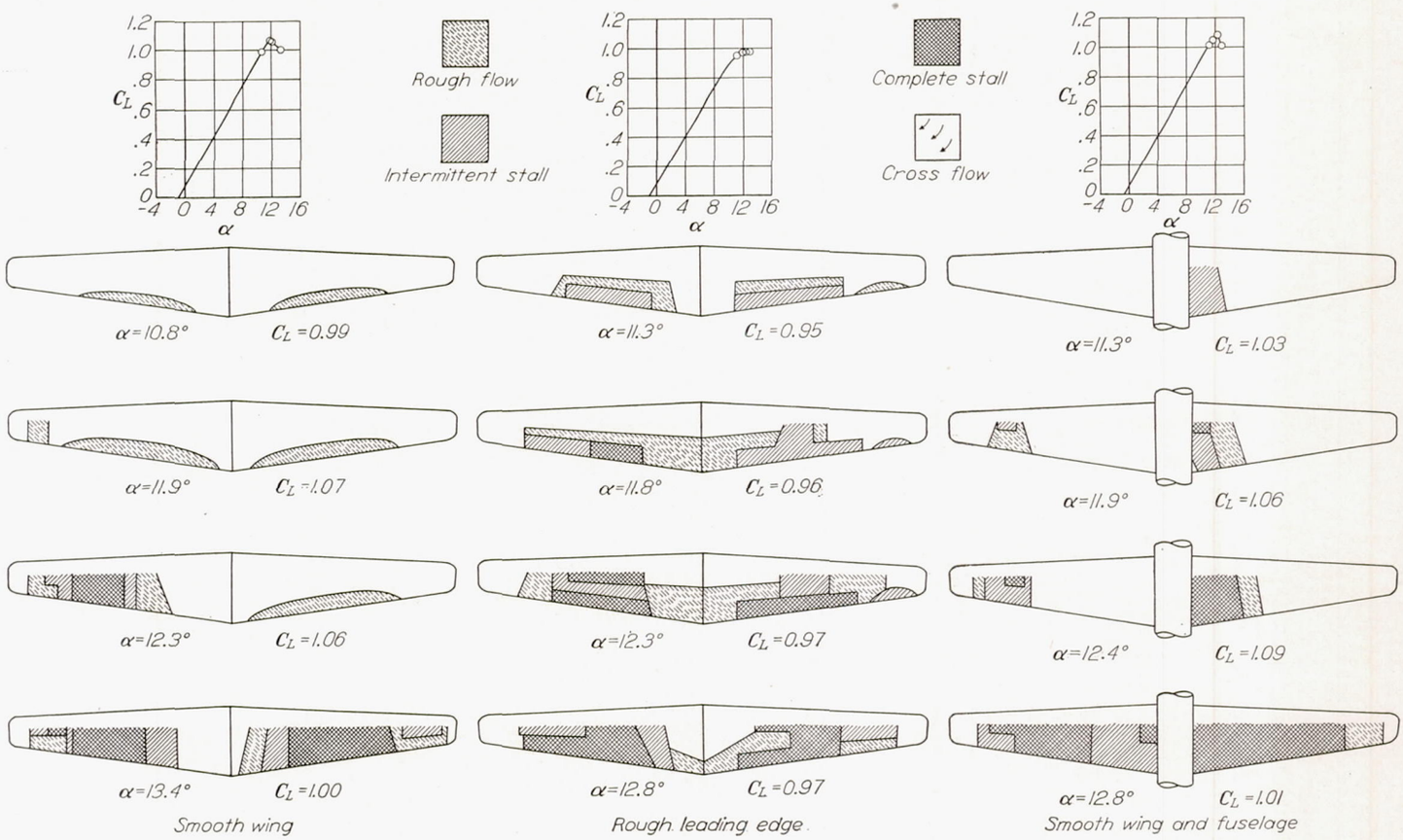

FIGURE 18.—Stalling characteristics of NACA 65-210 wing; flaps neutral. $R \approx 4{,}400{,}000$; $M \approx 0.17$.

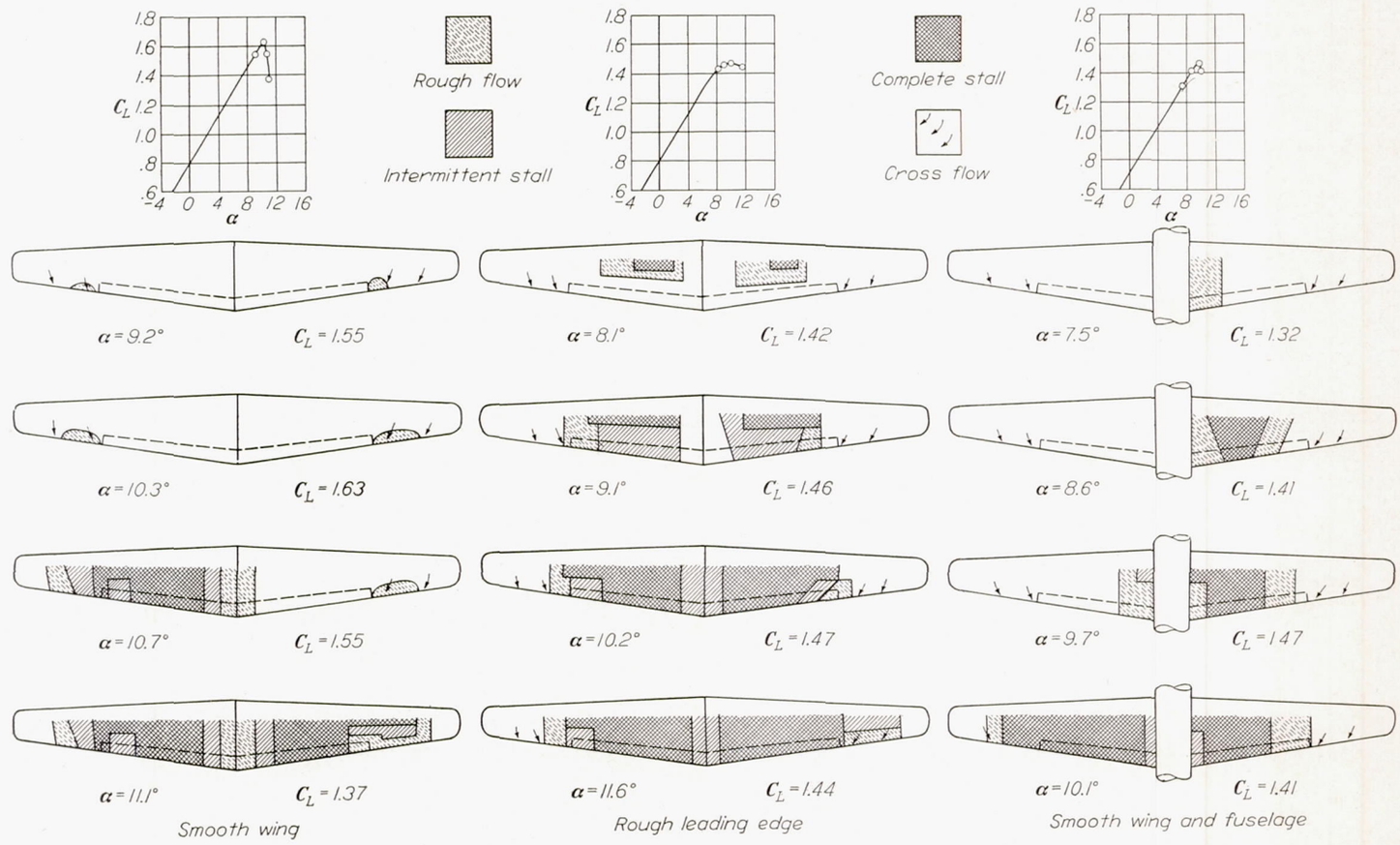

FIGURE 19.—Stalling characteristics of NACA 65-210 wing; partial-span split flaps. $R \approx 4{,}400{,}000$; $M \approx 0.17$.

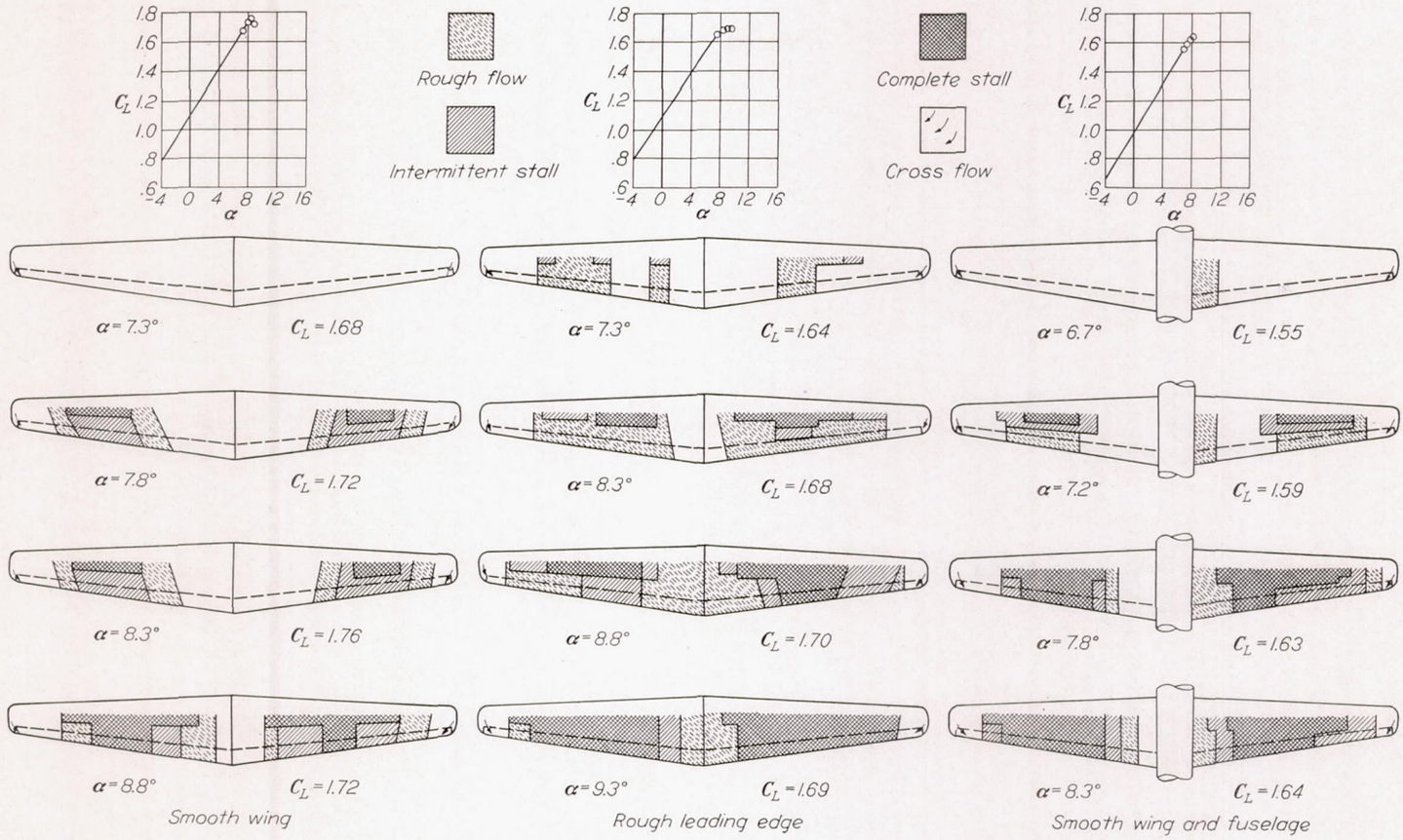

FIGURE 20.—Stalling characteristics of NACA 65-210 wing; full-span split flaps. $R \approx 4{,}400{,}000$; $M \approx 0.17$.

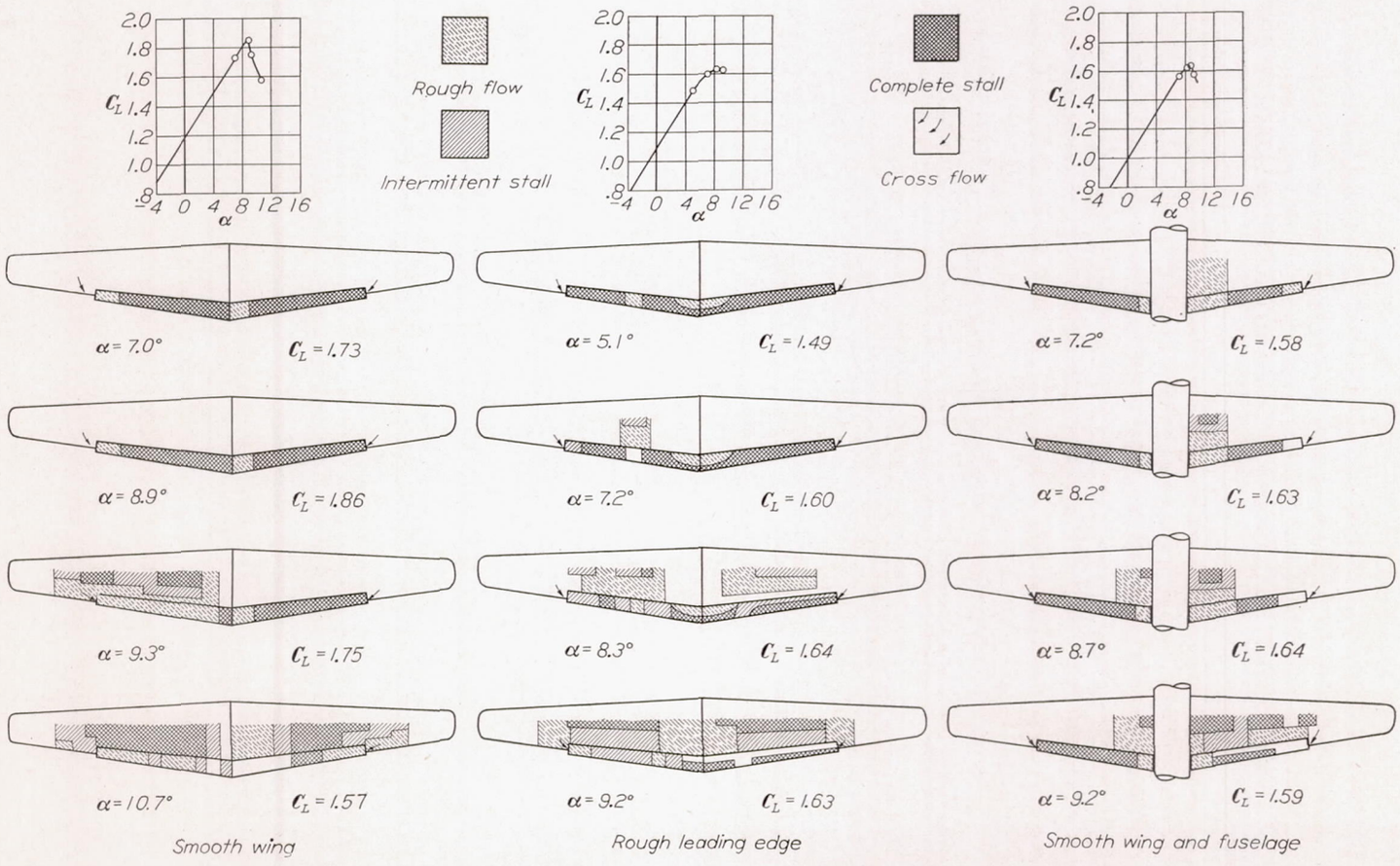

FIGURE 21.—Stalling characteristics of NACA 65-210 wing; partial-span single slotted flaps. $R \approx 4{,}400{,}000$; $M \approx 0.17$.

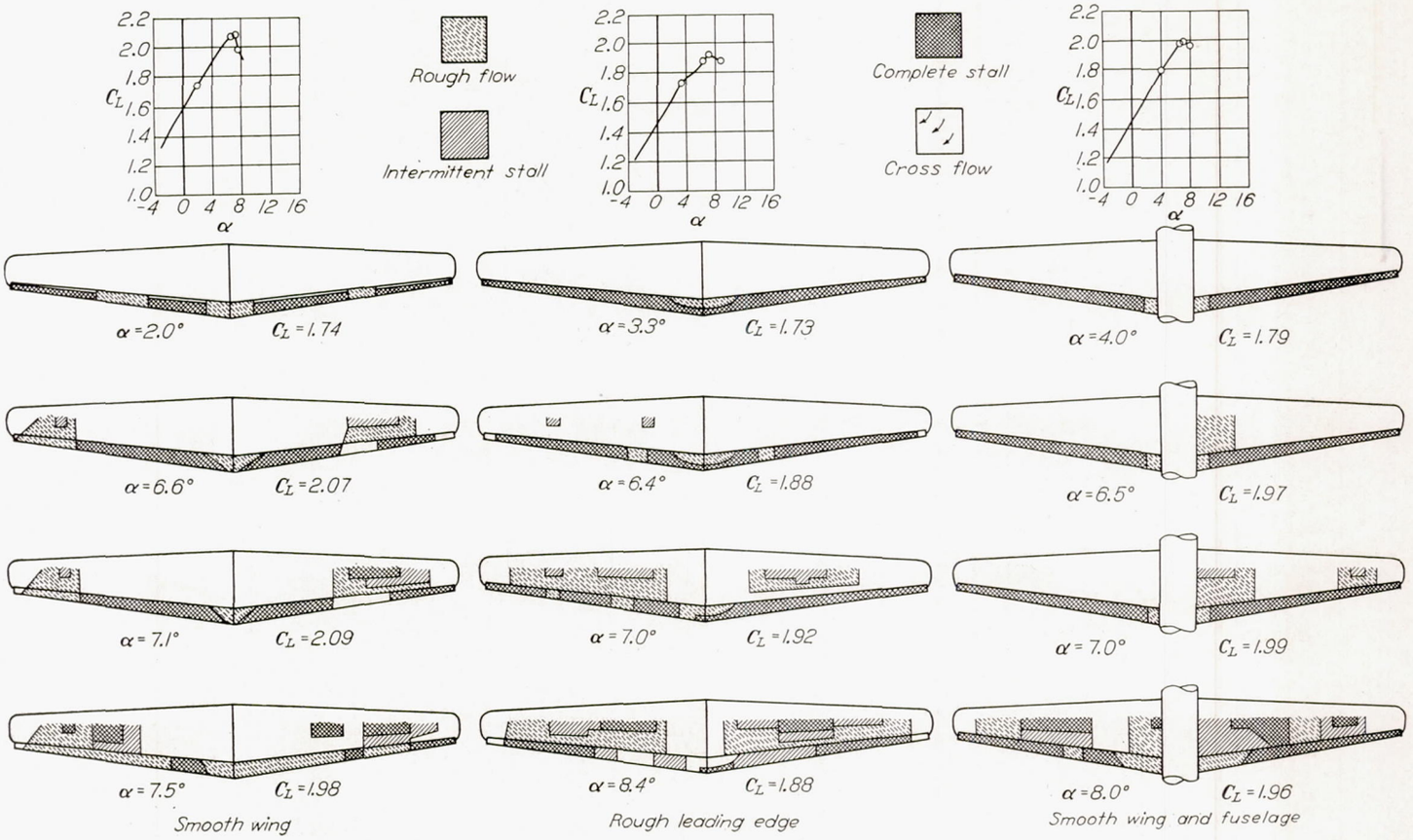

FIGURE 22.—Stalling characteristics of NACA 65–210 wing; full-span single slotted flaps. $R \approx 4{,}400{,}000$; $M \approx 0.17$.

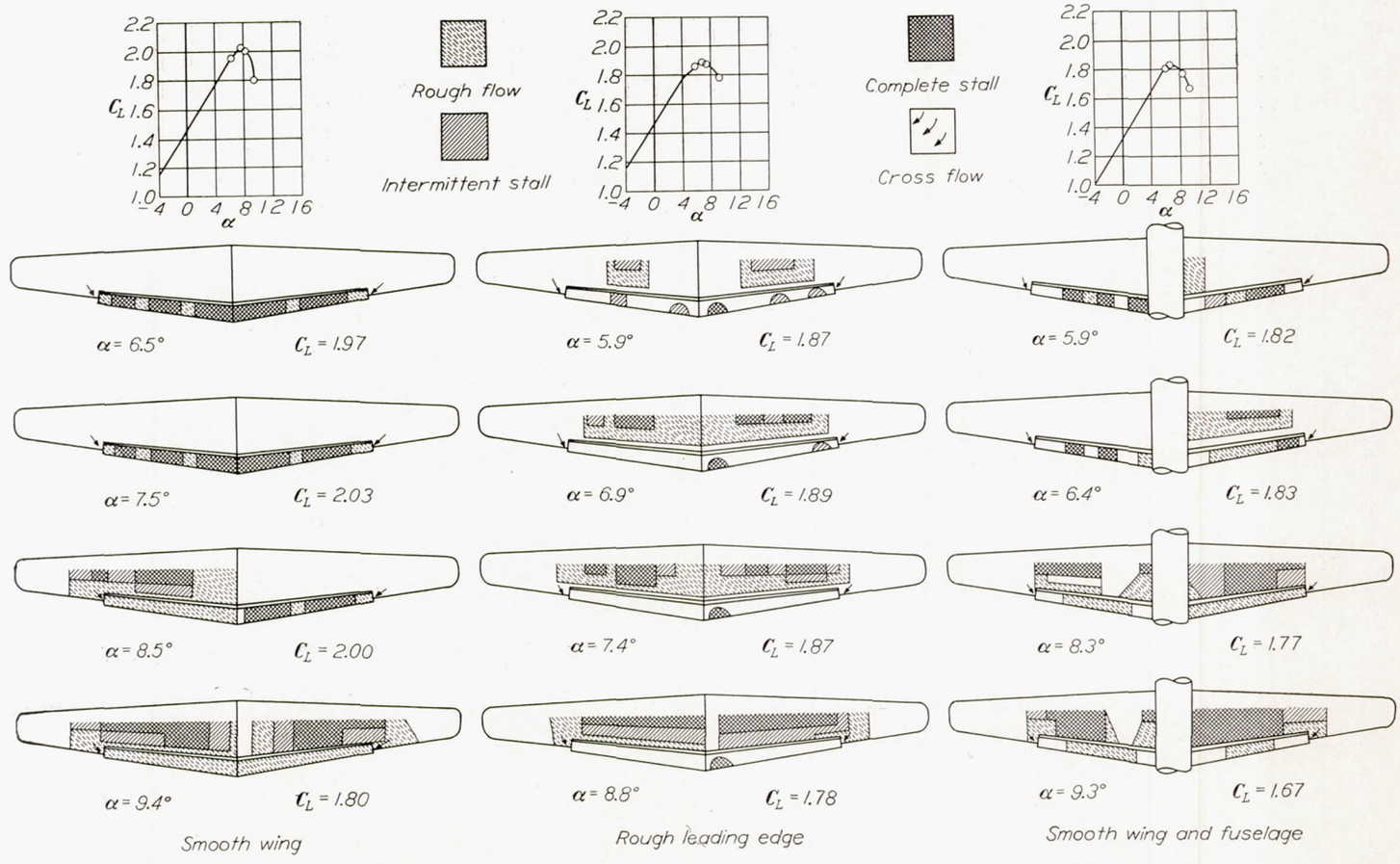

FIGURE 23.—Stalling characteristics of NACA 65–210 wing; partial-span double slotted flaps. $R \approx 4{,}400{,}000$; $M \approx 0.17$.

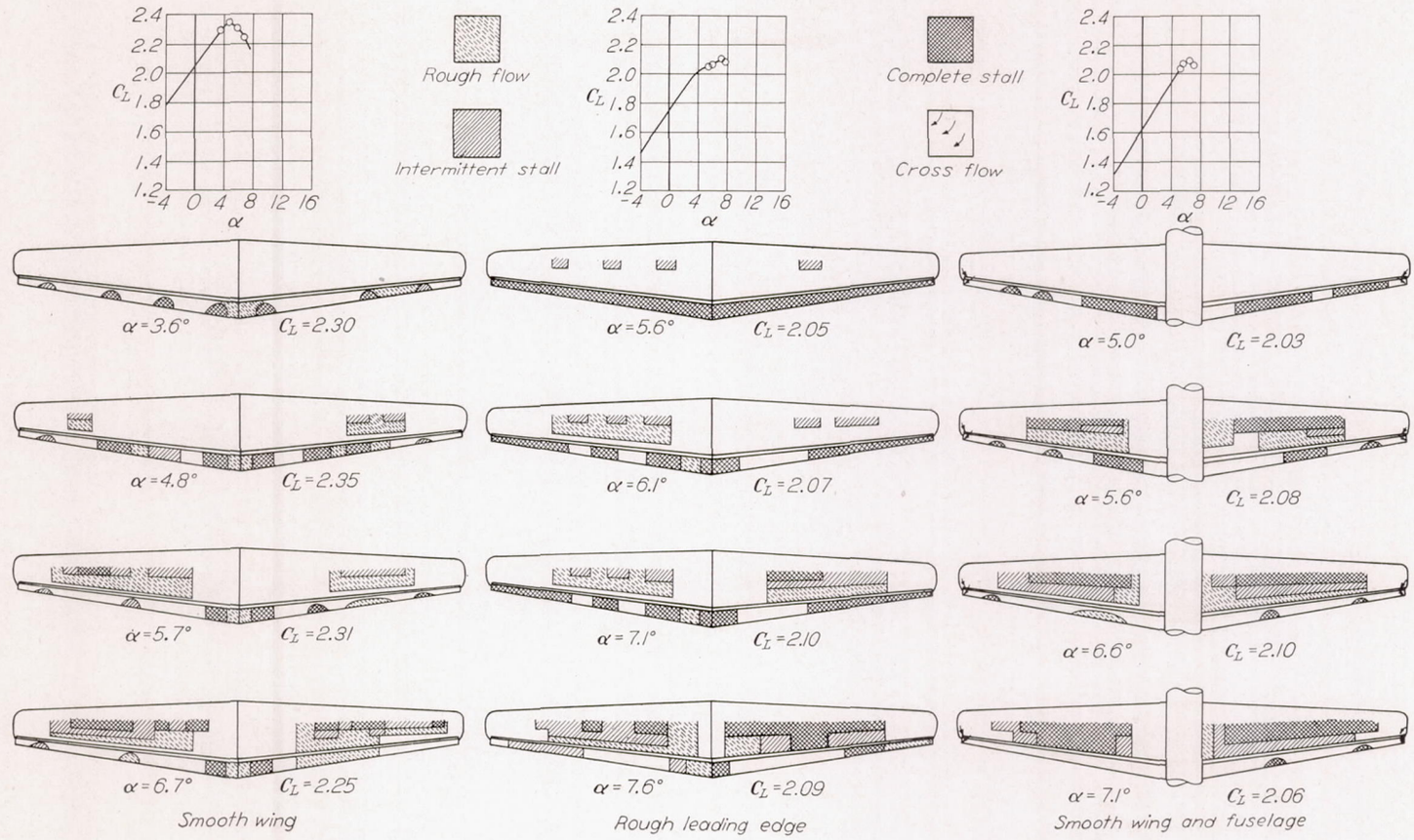

FIGURE 24.—Stalling characteristics of NACA 65–210 wing; full-span double slotted flaps. $R \approx$ 4,400,000; $M \approx$ 0.17.

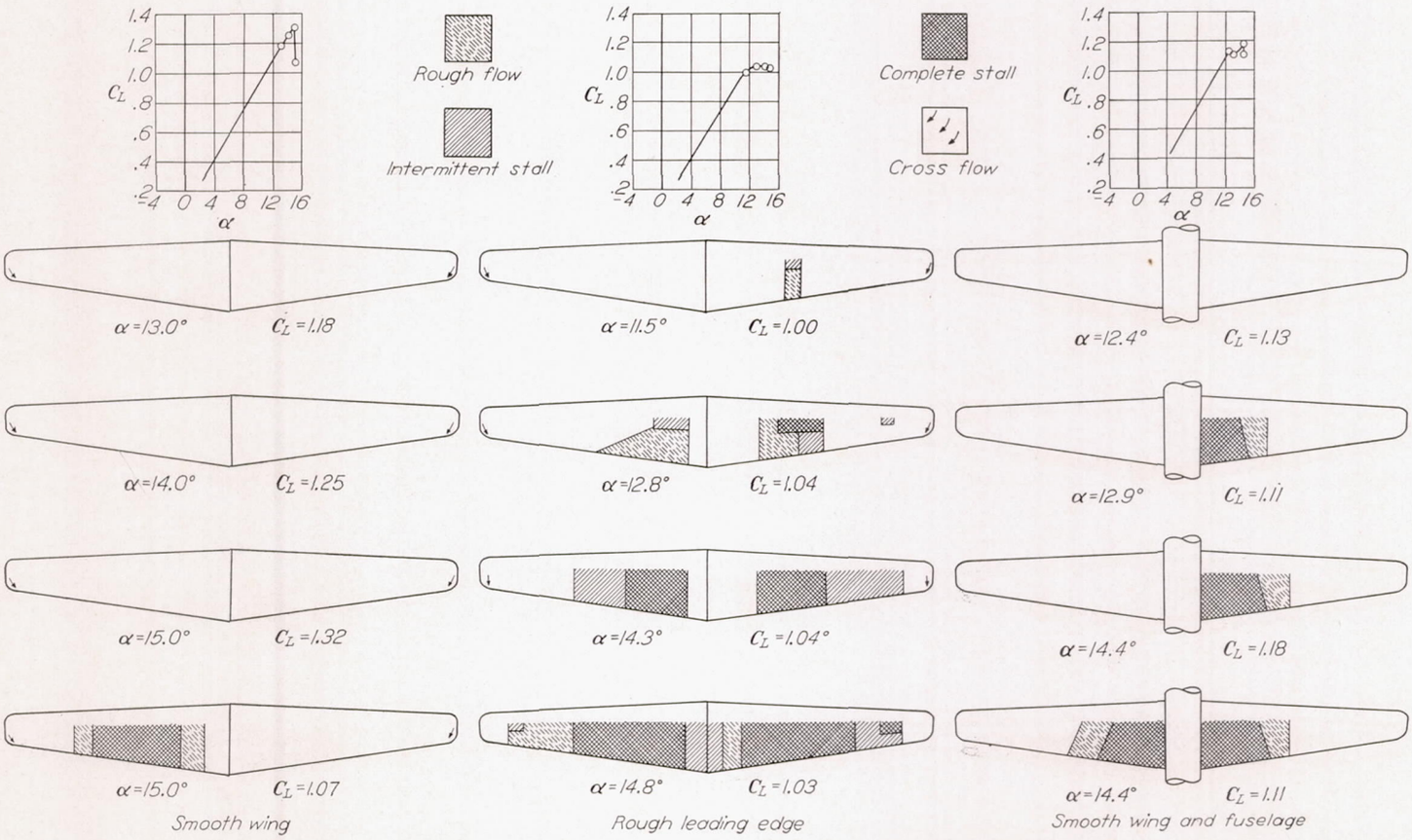

FIGURE 25.—Stalling characteristics of NACA 64–210 wing; flaps neutral. $R \approx$ 4,400,000; $M \approx$ 0.17.

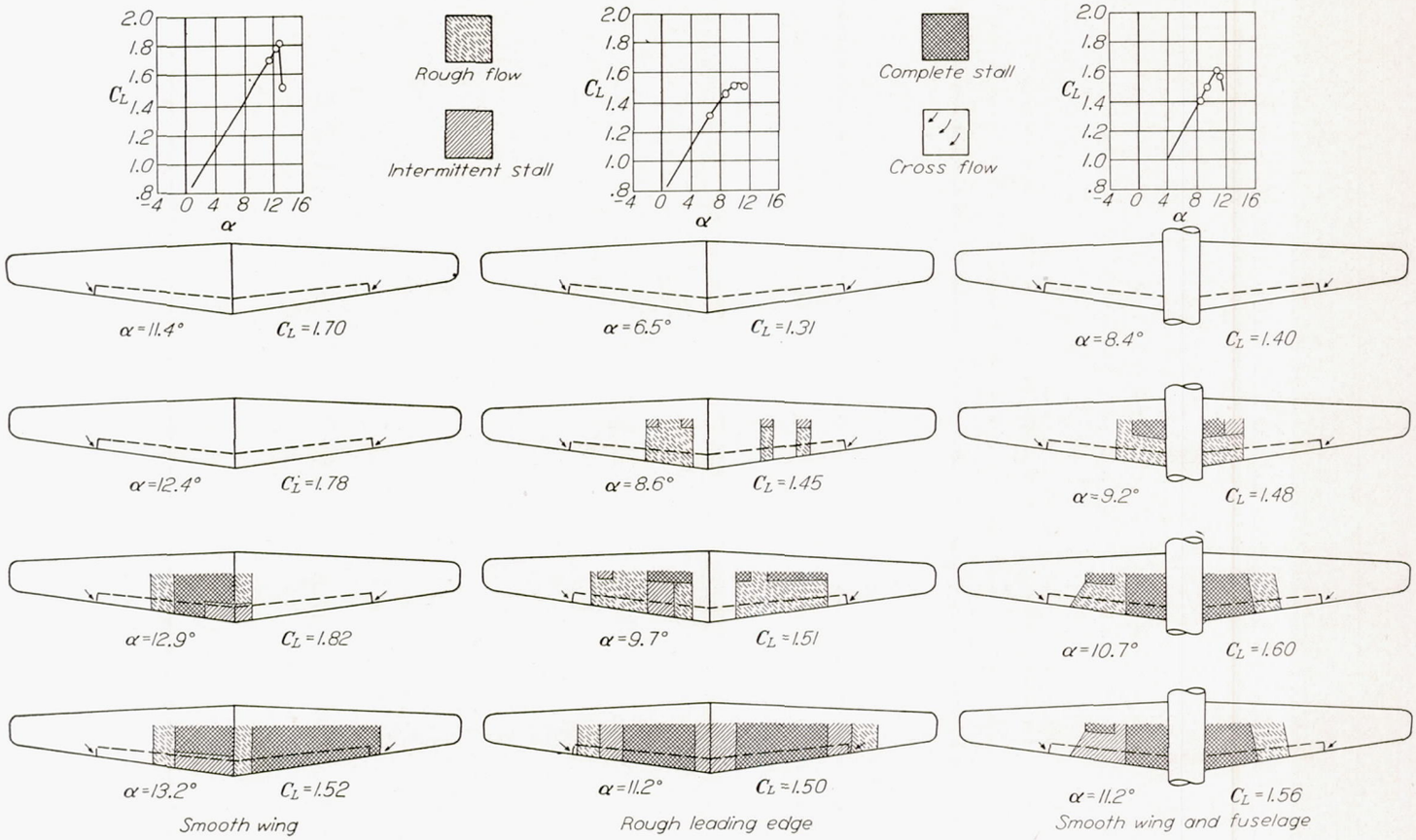

FIGURE 26.—Stalling characteristics of NACA 64–210 wing; partial-span split flaps. $R \approx$ 4,400,000; $M \approx$ 0.17.

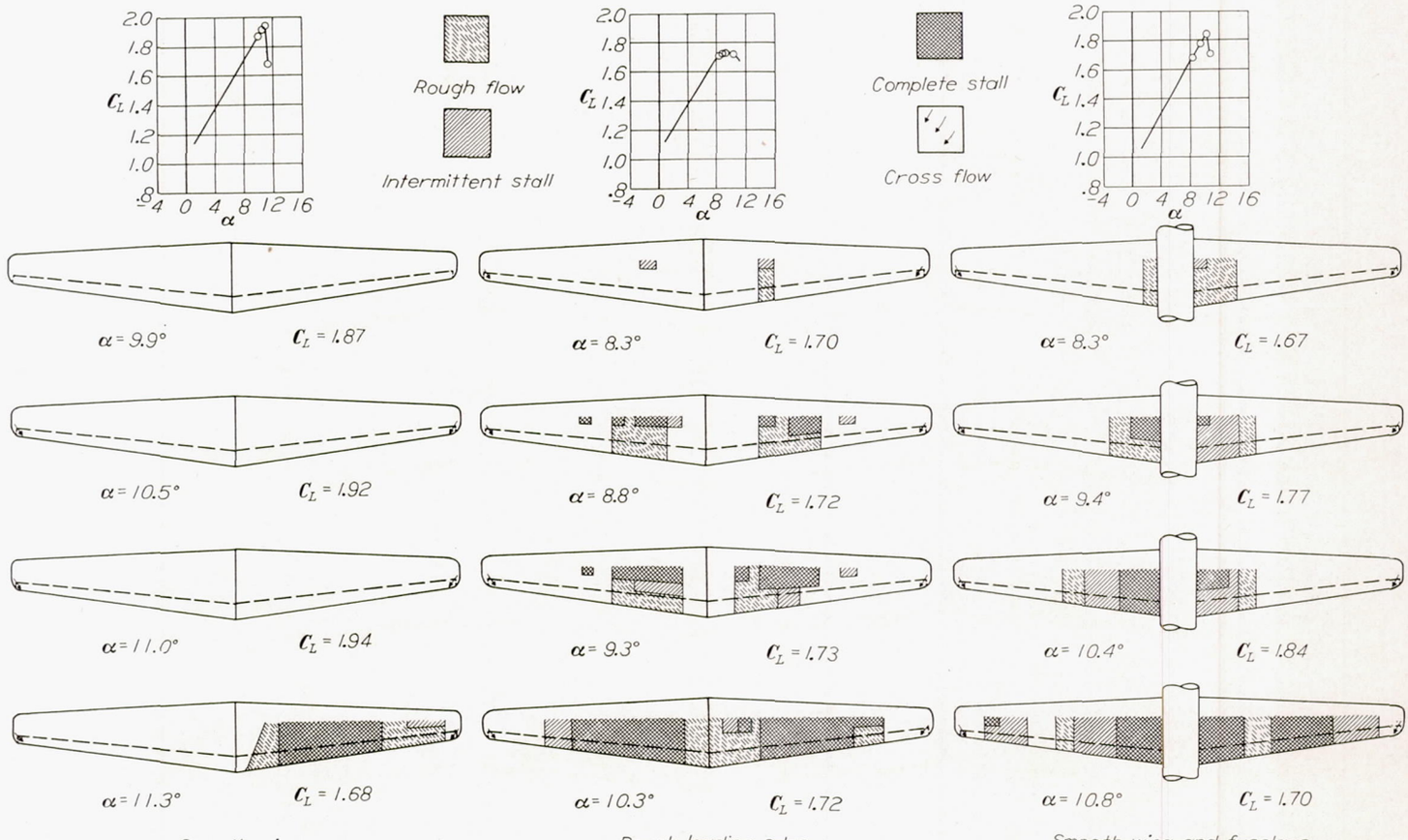

FIGURE 27.—Stalling characteristics of NACA 64–210 wing; full-span split flaps. $R \approx$ 4,400,000; $M \approx$ 0.17.

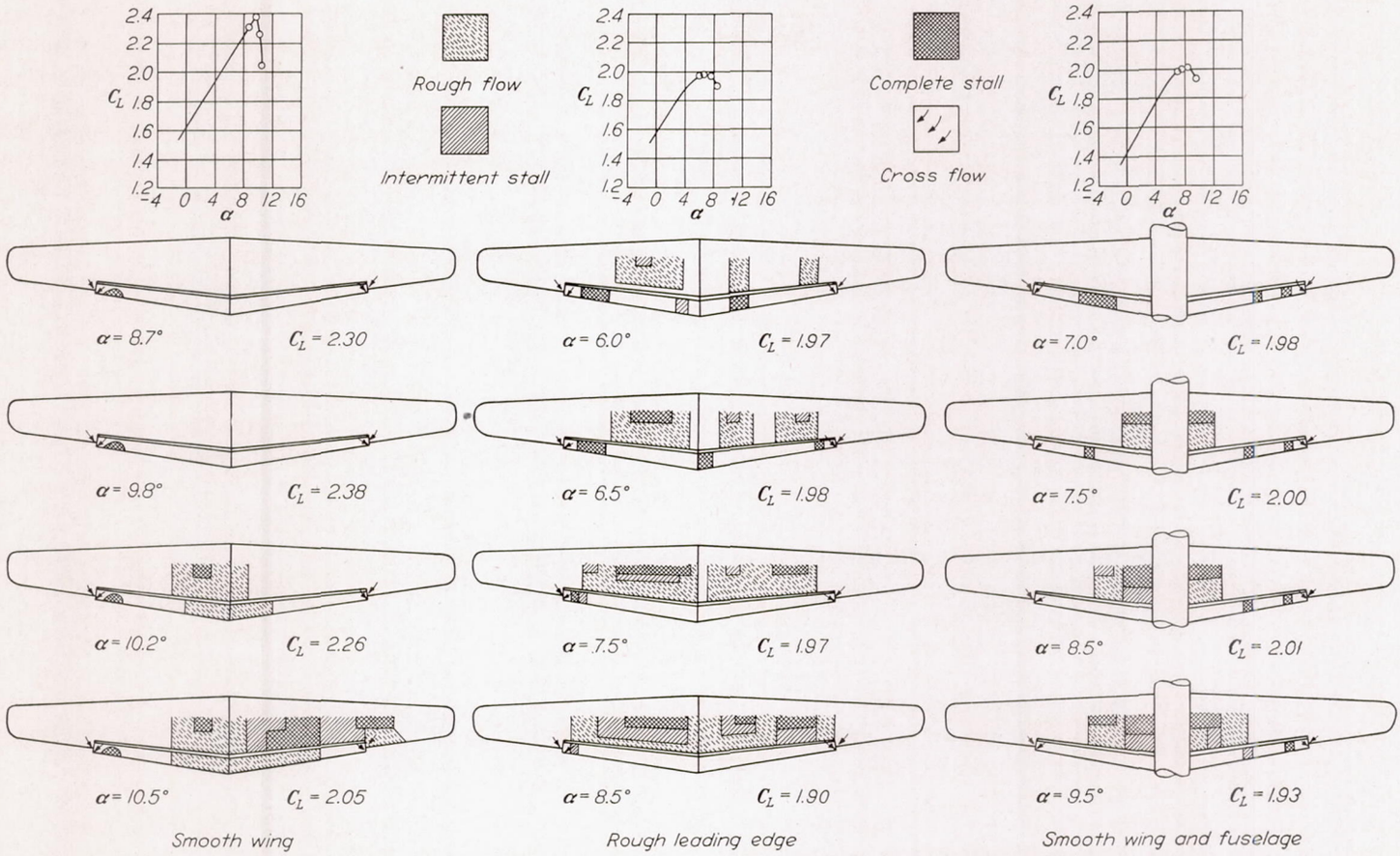

FIGURE 28.—Stalling characteristics of NACA 64–210 wing; partial-span double slotted flaps. $R \approx$ 4,400,000; $M \approx$ 0.17.

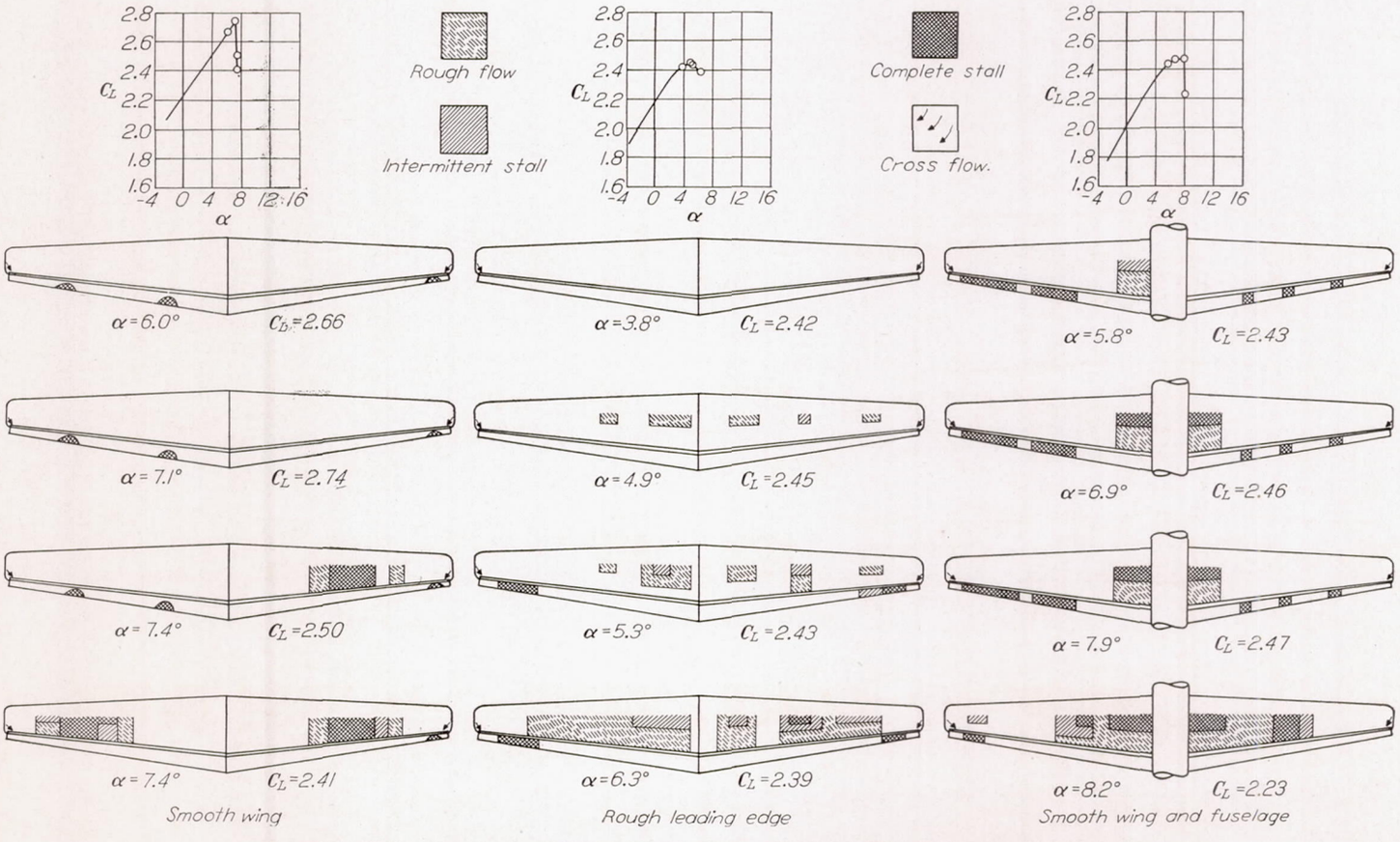

FIGURE 29.—Stalling characteristics of NACA 64-210 wing; full-span double slotted flaps. $R \approx$ 4,400,000; $M \approx$ 0.17.

STALLING CHARACTERISTICS

The stalling characteristics of the two wings as indicated by the tufts are shown in figures 18 to 29. The initial stall of these thin wings was characterized by an area of separated flow ahead of the 40-percent-chord line, with an area of unseparated flow behind it. An increase in angle of attack caused this area of stalled flow to extend rearward and spanwise in either direction. The unsymmetrical stall noted on many of the figures is typical of the inconsistency of the data near the maximum lift coefficient. On several repeat tests, either side of the wing was likely to stall first.

In general, the stall for the NACA 65–210 wing began between the 50-percent and 75-percent points of the semispan, whereas for the NACA 64–210 wing the stall began slightly more inboard. The NACA 64–210 wing stalled more abruptly and with greater loss of lift than did the NACA 65–210 wing. However, because the tips remained freer of stalled area, the aileron effectiveness of this wing would probably be better maintained beyond maximum lift than for the NACA 65–210 wing.

The pattern of the stall was little affected by flaps or leading-edge roughness, but the progression of the stall was more gradual with roughness. The fuselage caused a premature stall to start near the wing-fuselage junction. This premature stall might have been eliminated by properly designed fillets, thereby increasing the maximum lift coefficient. The presence of this stall, however, might produce tail buffeting which would warn the pilot of the impending stall and also provide longitudinal stability at the stall for the single-slotted-flap and double-slotted-flap configurations.

CONCLUSIONS

From the results of tests in the Langley 19-foot pressure tunnel of a wing with NACA 65–210 airfoil sections and a wing with NACA 64–210 airfoil sections with several types of flaps, the following conclusions may be drawn:

1. At a Reynolds number of 4,400,000 maximum lift coefficients of 2.48 and 2.76, respectively, were obtained with the NACA 65–210 and 64–210 wings with full-span double slotted flaps. These values are approximately 205 percent of the flap neutral values of 1.21 and 1.35 for the respective wings.

2. Addition of the fuselage or the leading-edge roughness caused reductions of 0.1 to 0.3 in the maximum lift coefficients of the wings. The NACA 64–210 wing was affected to a greater extent than was the NACA 65–210 wing, although the maximum lift coefficients for the NACA 64–210 wing were still higher.

3. Increases in maximum lift coefficient with increases in Reynolds number were obtained at Reynolds numbers below 4,400,000. Above this value, the test Mach number was high enough so that the effects of compressibility appeared to be a contributing factor in causing maximum lift coefficients to increase less rapidly or to decrease with increasing Reynolds number.

4. The stall of the NACA 64–210 wing was somewhat more abrupt but slightly farther inboard than that of the NACA 65–210 wing. The pattern of stall was not appreciably altered by the leading-edge roughness or by the various flap configurations. The fuselage, however, caused the stall to begin inboard near the wing-fuselage junction.

LANGLEY MEMORIAL AERONAUTICAL LABORATORY,
NATIONAL ADVISORY COMMITTEE FOR AERONAUTICS,
LANGLEY FIELD, VA., *August 19, 1947.*

REFERENCES

1. Cahill, Jones F.: Two-Dimensional Wind-Tunnel Investigation of Four Types of High-Lift Flap on an NACA 65–210 Airfoil Section. NACA TN 1191, 1947.
2. Cahill, Jones F., and Racisz, Stanley F.: Wind-Tunnel Investigation of Seven Thin NACA Airfoil Sections to Determine Optimum Double-Slotted-Flap Configurations. NACA TN 1545, 1948.
3. Furlong, G. Chester, and Fitzpatrick, James E.: Effects of Mach Number and Reynolds Number on the Maximum Lift Coefficient of a Wing of NACA 230-Series Airfoil Sections. NACA TN 1299, 1947.

TABLE I

ORDINATES FOR NACA 65–210 AIRFOIL

[Stations and ordinates given in percent airfoil chord]

Upper surface		Lower surface	
Station	Ordinate	Station	Ordinate
0	0	0	0
.435	.819	.565	−.719
.678	.999	.822	−.859
1.169	1.273	1.331	−1.059
2.408	1.757	2.592	−1.385
4.898	2.491	5.102	−1.859
7.394	3.069	7.606	−2.221
9.894	3.555	10.106	−2.521
14.899	4.338	15.101	−2.992
19.909	4.938	20.091	−3.346
24.921	5.397	25.079	−3.607
29.936	5.732	30.064	−3.788
34.951	5.954	35.049	−3.894
39.968	6.067	40.032	−3.925
44.984	6.058	45.016	−3.868
50.000	5.915	50.000	−3.709
55.014	5.625	54.986	−3.435
60.027	5.217	59.973	−3.075
65.036	4.712	64.964	−2.652
70.043	4.128	69.957	−2.184
75.045	3.479	74.955	−1.689
80.044	2.783	79.956	−1.191
85.038	2.057	84.962	−.711
90.028	1.327	89.972	−.293
95.014	.622	94.986	.010
100.000	.050	100.000	−.050

L. E. radius: 0.687.
Slope of radius through L. E.: 0.084.

TABLE II

ORDINATES FOR NACA 64–210 AIRFOIL

[Stations and ordinates given in percent airfoil chord]

Upper surface		Lower surface	
Station	Ordinate	Station	Ordinate
0	0	0	0
.431	.867	.569	−.767
.673	1.056	.827	−.916
1.163	1.354	1.337	−1.140
2.401	1.884	2.599	−1.512
4.890	2.656	5.110	−2.024
7.387	3.248	7.613	−2.400
9.887	3.736	10.113	−2.702
14.894	4.514	15.106	−3.168
19.905	5.097	20.095	−3.505
24.919	5.533	25.081	−3.743
29.934	5.836	30.066	−3.892
34.951	6.010	35.049	−3.950
39.968	6.059	40.032	−3.917
44.985	5.938	45.015	−3.748
50.000	5.689	50.000	−3.483
55.014	5.333	54.987	−3.143
60.025	4.891	59.975	−2.749
65.033	4.375	64.967	−2.315
70.038	3.799	69.962	−1.855
75.040	3.176	74.960	−1.386
80.038	2.518	79.962	−.926
85.033	1.849	84.968	−.503
90.024	1.188	89.977	−.154
95.012	.564	94.988	.068
100.000	.050	100.000	−.050

L. E. radius: 0.720.
Slope of radius through L. E.: 0.084.

TABLE III

FLAP ORDINATES FOR NACA 65–210 AIRFOIL

[Stations and ordinates given from flap chord line in percent airfoil chord]

Upper surface		Lower surface	
Station	Ordinate	Station	Ordinate
0	0	0	0
.28	.92	.28	−.41
.56	1.19	.56	−.62
1.12	1.56	1.12	−.88
1.69	1.83	1.69	−1.00
2.22	1.99	2.48	−1.03
3.38	2.22	4.98	−.83
4.50	2.33	7.48	−.63
5.61	2.38	9.98	−.44
7.00	2.40	12.48	−.27
9.00	2.35	14.98	−.12
11.00	2.16	17.48	.01
12.51	1.91	19.99	.10
15.01	1.50	22.49	.12
17.51	1.10	25.00	−.05
20.00	.711		
22.50	.341		
25.00	.05		

L. E. radius: 0.800.
L. E. radius center: 0.240 above flap chord line.

TABLE IV

FLAP ORDINATES FOR NACA 64-210 AIRFOIL

[Stations and ordinates given from flap chord line in percent airfoil chord]

Upper surface		Lower surface	
Station	Ordinate	Station	Ordinate
0	0	0	0
.25	.78	.25	−.34
.50	1.01	.50	−.50
1.00	1.32	1.00	−.70
2.00	1.69	2.00	−.90
3.00	1.89	2.50	−.90
4.00	2.01	4.95	−.70
5.00	2.07	9.96	−.33
6.00	2.09	14.98	−.04
7.00	2.09	19.99	.13
9.00	2.05	25.00	−.05
11.00	1.88		
15.04	1.30		
20.02	.62		
25.00	.05		

L. E. radius: 0.620.
L. E. radius center: 0.170 above flap chord line.

TABLE V

ORDINATES FOR 0.075 CHORD VANE

[Stations and ordinates given from vane chord line in percent airfoil chord]

Station	Upper ordinate	Lower ordinate
0	0	0
.42	.95	−.93
.83	1.31	−1.14
1.25	1.52	−1.20
1.67	1.62	−1.11
2.08	1.72	−.85
2.92	1.74	−.36
3.75	1.64	−.02
4.58	1.43	.18
5.42	1.13	.27
6.25	.75	.25
7.08	.28	.11
7.50	0	0

L. E. radius: 1.20 (on chord line).

TABLE VI

ORDINATES FOR UPPER SURFACE OF FLAP WELL

[Stations and ordinates given from airfoil chord line in percent airfoil chord]

Station	Ordinate NACA 65–210 airfoil	Ordinate NACA 64–210 airfoil
74.75	−0.40	−0.29
75.00	.36	.43
76.00	1.24	1.20
77.00	1.70	1.60
78.00	2.00	1.86
79.00	2.19	2.02
79.75	2.30	2.11
84.00	2.16	1.94

Ordinates between stations 79.75 and 84.00 connected by straight lines.

TABLE VII

SUMMARY OF RESULTS OBTAINED FROM TESTS IN LANGLEY 19-FOOT PRESSURE TUNNEL OF TWO WINGS, ONE INCORPORATING NACA 65–210 AIRFOIL SECTIONS, THE OTHER, NACA 64–210 AIRFOIL SECTIONS. $R \approx 4{,}400{,}000$; $M \approx 0.17$.

Flap type	Flap span	Smooth Wing				Wing with fuselage		Wing with roughness	
		$C_{L_{max}}$		$C_{L_{max_{trim}}}$		$C_{L_{max}}$		$C_{L_{max}}$	
		65–210 wing	64–210 wing	65–210 wing	64–210 wing	65–210 wing	64–210 wing	65–210 wing	64–210 wing
Flaps neutral		1.21	1.35	1.20	1.34	1.12	1.17	0.99	1.05
Split	Partial	1.63	1.87	1.57	1.81	1.48	1.58	1.49	1.52
	Full	1.74	1.94	1.66	1.87	1.64	1.86	1.70	1.73
Slotted	Partial	1.87	------	1.75	------	1.77	------	1.70	------
	Full	2.15	------	2.00	------	2.01	------	1.98	------
Double slotted	Partial	2.10	2.42	1.94	2.26	2.01	2.09	1.86	2.02
	Full	2.48	2.76	2.27	2.55	2.34	2.53	2.28	2.48

U. S. GOVERNMENT PRINTING OFFICE: 1950

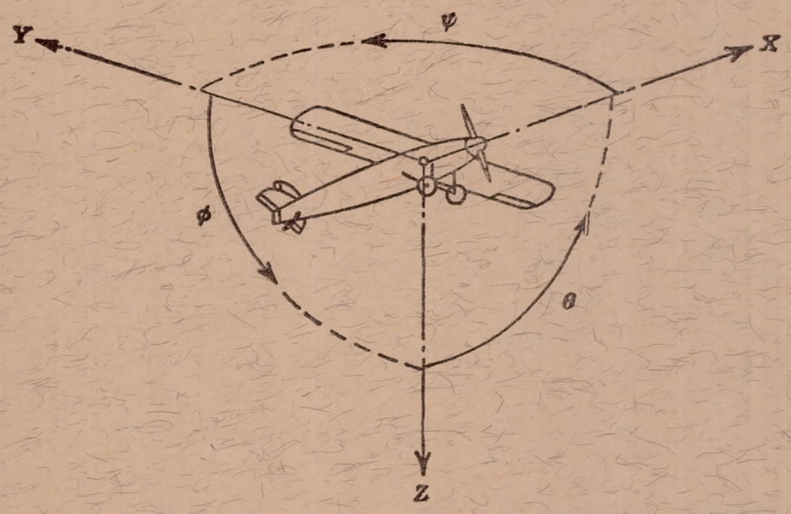

Positive directions of axes and angles (forces and moments) are shown by arrows

Axis		Force (parallel to axis) symbol	Moment about axis			Angle		Velocities	
Designation	Symbol		Designation	Symbol	Positive direction	Designation	Symbol	Linear (component along axis)	Angular
Longitudinal	X	X	Rolling	L	$Y \longrightarrow Z$	Roll	ϕ	u	p
Lateral	Y	Y	Pitching	M	$Z \longrightarrow X$	Pitch	θ	v	q
Normal	Z	Z	Yawing	N	$X \longrightarrow Y$	Yaw	ψ	w	r

Absolute coefficients of moment

$C_l = \frac{L}{qbS}$ (rolling) $\quad C_m = \frac{M}{qcS}$ (pitching) $\quad C_n = \frac{N}{qbS}$ (yawing)

Angle of set of control surface (relative to neutral position), δ. (Indicate surface by proper subscript.)

4. PROPELLER SYMBOLS

D Diameter

p Geometric pitch

p/D Pitch ratio

V' Inflow velocity

V_s Slipstream velocity

T Thrust, absolute coefficient $C_T = \frac{T}{\rho n^2 D^4}$

Q Torque, absolute coefficient $C_Q = \frac{Q}{\rho n^2 D^5}$

P Power, absolute coefficient $C_P = \frac{P}{\rho n^3 D^5}$

C_s Speed-power coefficient $= \sqrt[5]{\frac{\rho V^5}{P n^2}}$

η Efficiency

n Revolutions per second, rps

Φ Effective helix angle $= \tan^{-1}\left(\frac{V}{2\pi r n}\right)$

5. NUMERICAL RELATIONS

1 hp=76.04 kg-m/s=550 ft-lb/sec

1 metric horsepower=0.9863 hp

1 mph=0.4470 mps

1 mps=2.2369 mph

1 lb=0.4536 kg

1 kg=2.2046 lb

1 mi=1,609.35 m=5,280 ft

1 m=3.2808 ft